11

MODELING OF P-T-t PATHS CONSTRAINED BY MINERAL CHEMISTRY AND MONAZITE DATING OF METAPELITES IN RELATIONSHIP TO MCT ACTIVITY IN SIKKIM, EASTERN HIMALAYAS

CHANDRA S. DUBEY*, E.J. CATLOS** AND B.K. SHARMA*

ABSTRACT

The metapelites of lesser Himalaya in Sikkim underwent two phases of prograde metamorphism, each culminating into a retrograde metamorphic episode. The first event was prograde regional metamorphism, M_1, during which S_1 and S_2 schistosity were developed. During this episode of metamorphism of chlorite, chloritoid, biotite, garnet, staurolite and kyanite were formed. Most of the prograde minerals (chlorite to staurolite) in this phase of metamorphism were formed by continuous reactions. Different geothermometers revealed temperatures upto 465 to 527°C in garnet zone and 555 to 576°C (Core parts) in staurolite zone. The maximum pressure in core of garnets in staurolite zone was inferred upto 6.6Kbr.

The M_1 metamorphism was followed by a retrogressive phase M_{1a} due to which the prograde minerals from chlorite to kyanite showed alteration effects. The temperatures and pressure of this retrogressive event is inferred from outer core parts of garnets in staurolite zone from 492 to 522°C at 5.7Kbr pressure.

M_2, metamorphism was again a prograde type during which garnet, staurolite, kyanite and sillimanite (with almandine) were formed. The temperature and pressure during M_2 metamorphic phase reached in the range of 630 to 695°C at 6.9-7.3Kbr respectively in kyanite-sillimanite zone. The metamorphic episode M_2 again culminated into retrograde metamorphism M_{2a}, during which the rims of the multistage garnet were chloritised. The other evidences are replacement of k-rich feldspar by muscovite, reverse zoning of garnet at rim, pseudomorph of chlorite after idioblastic garnet, decrease in Zn content of staurolite.

In the Sikkim Himalaya, inverted metamorphism is the characteristics of rocks that underlie the MCT zone. Monazites dated in the thin section indicate that the Sikkim Himalayan MCT shear zone was active during 22-20Ma and 14-10Ma. The ages indicate inverted metamorphism generated via accretion of successive tectonic slivers of the Lesser Himalaya to the hanging wall. The paper outlines a model for the development of the Sikkim Himalayas based on P-T-t paths.

* Department of Geology, University of Delhi, Delhi-110007, India

** School of Geology, Oklahoma State University, Stillwater, OK, USA

Metamorphism and Crustal Evolution: Eds. H. Thomas. Atlantic Pub. 2005

KEYWORDS

Mineral Chemistry; Monazite dating, MCT and P-T-t paths.

INTRODUCTION

The Sikkim Himalaya is tectonically characterised by a domal structure on regional scale and the eastern half of domal structure in Eastern Himalaya (Sikkim) has been studied (Fig. 1A &1B). Gansser (1964) opined that the gneisses were tectonically emplaced in the Dalings and were not related to the Darjeeling gneiss. Banerjee *et al.* (1980), based on landsat and Air photos, marked that the area witnessed differential uplift along a number of regional and local sub-vertical faults. Chloritic slates of the Dalings merged imperceptibly through biotite schists to garnet and staurolite schists of the Darjeeling group. Banerjee and Bhattacharya (1981) considered that there was an absence of prograde chloritoid and cordierite in the metamorphites of Sikkim and these minerals were locally formed as retrograde products of prograde assemblages.

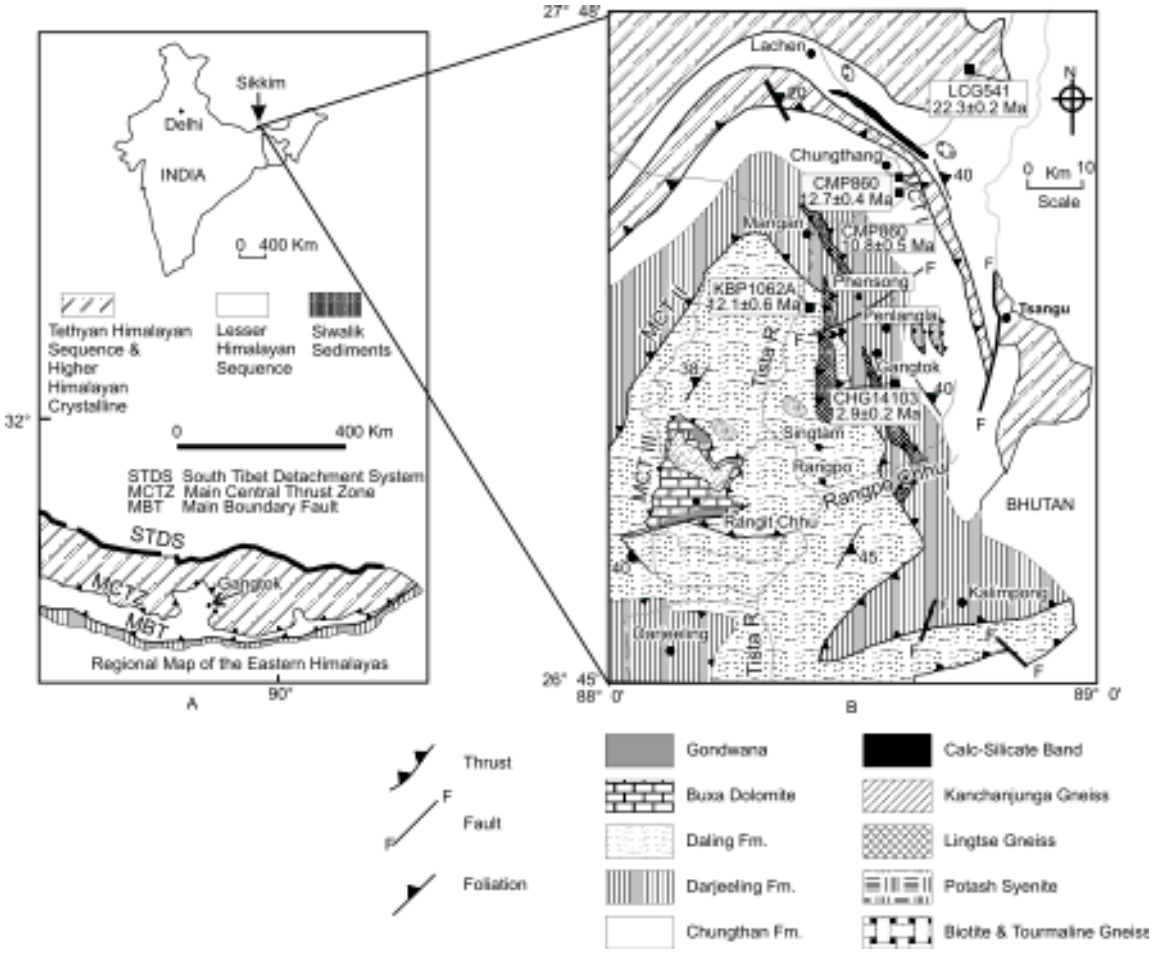

Fig. 1. Geological map of Sikkim (Eastern Himalaya).

Geological Setting

The Himalayan sequence of Sikkim consists of various lithostratigraphic units from low to high metamorphic grades. Igneous rocks occur as intrusives (potassic syenite, *i.e.* Sikkim Fm) in the Daling near Khamdong and Singtam. Stratigraphically these rocks have been grouped into Chungthang-Darjeeling-, Daling-, Lingtse- (Acharyya, 1989) and Sikkim igneous Formation (Dubey, 1993). The contact between Darjeeling and Daling near Deorali is a sheared one and the rocks are highly mylonitised along the contact especially near Deorali. The streaky biotite gneiss (Lingtse) occurs in the form of bands which are present within the low grade Daling and medium to high grade Darjeeling Formations. The Lingtse gneiss is characterized by sheared contacts with Darjeeling and Daling Formations. Chungthang and Darjeeling Fromations are the part of Higher Himalayan Crystalline and Daling Formation is Lesser Himalayan low grade metamorphites (Fig. 1B).

The regional strikes of lithological units are NW-SE dipping 20-65° towards NE. However, in the southern part, gradually changes to NE-SW with 30-65° of dips in SE (*e.g.* along Rangpo-Melli, Rangpo-Rongli and Rangpo-Singtam roads). Local variation in the strike-trend can be attributed to deformation specially observed near Singtam and Rumtek.

Detail description of rocks unit are described on the basis of field relationship, geographical location, megascopic characteristics, texture, colour composition grain size and shape etc. All the rock units are described in detail keeping in view the geographical distribution, field relations, textures, grain size, shape, colour, composition, etc (Dubey, 1993).

Chungthang Formation

Chungthang Formation is highly deformed, metamorphosed and mainly consists of calc-quartzites, calc-silicates, calc granulites and gneisses. Retrogression effect was observed in the gneisses. The presence of retrograde pennine chlorite, coarse porphyroclast of quartz, ribbon quartz and sheared bands/anatomizing shear zone in calcareous quartzites depicts evidence of shearing and thrusting.

Darjeeling Formation

The Darjeeling Formation consists of medium to high grade metamorphic rocks and shows gradational contact with Daling metamorphites. The Darjeeling Formation comprises of migmatitic gneisses, kyanite-sillimanite zone (kyanite-silliminite schist, kyanite gneiss, kyanite-staurolite schist), staurolite zone (staurolite-garnet-schist) and garnet zone (garnet schist) associated with bands of amphibolite. The staurolite-garnet and garnet schist form the lower members of the Darjeeling Formation depicting prominent effects of retrogression shearing and mylonitisation.

Daling Formation

The Daling Formation covers a large part of area from Melli-Rangpo in south to Dikchu and from west of Singtam (Tumin) to Rumtek in the east and gradational contact has been observed on National Highway 31A in between Martam and Ranipul village. Daling Formation comprises of chloritoid schist and phyllite intercalated with quartzites belongs to chloritoid and chlorite zones.

Tectonics

The rock units exposed in Sikkim Himalaya have been multiply deformed and metamorphosed in due course of time. The three phase of deformation have been observed

during the field investigations which are substantiated by the microstructural evidences. The Sikkim area is tectonically delineated by well defined thrusts *i.e.* the Main Central Thrust (shear zone) which brings the migmatites and gneisses over the medium to high grade schists and gneisses (Darjeeling formation) and also depicts tectonic contacts with the Lingtse gneiss and low grade Daling phyllites. During the last stage of deformation (D_3), the rocks were affected by thrusting acquired domal structure.

Main Central Thrust (MCT-I) equivalent to the Vaikrita Thrust could be recognized in the northern part of the area where the Greater Himalayan Crystalline Complex is separated abruptly close to Chungthang by calc rich quartzites, calc silicates and calc granulites. Highly sheared and retrograded calcareous quartzites (Fig. 2A) calc silicated and calc granulites are observed 2Km South of Chungthang (Fig. 1B). The shear fabrics L-S dominates, the calcareous quartzites and is clearly replaced by the flattening fabric of the Greater Himalayan Crystalline Complex in the north (Pecher, 1989). The position of MCT-II close to the MCT-I is marked in the south of Gangtok in the mylonitic Lingtse gneiss (Fig. 2B), retrograded staurolite and garnet bearing schists which overly the low grade Lesser Himalayan Formation at Martam. MCT-II of Sikkim Himalaya is recognized as Munsiari Thrust in the Garhwal Himalaya and could be related to MCT-I in Nepal (Arita, 1983). MCT-I and MCT-II is separated by the wide shear zone of strongly to weakly metamorphosed rocks of Darjeeling and Daling Formation along with thrust slice wedges of sheared Lingtse gneiss (Fig. 1B). MCT-III is recognized as Rangit Thrust by previous workers (Acharyya, 1989; Banerjee *et al.*, 1980; Sinha Roy, 1977). The dips of the foliation S_2 are recorded in one direction mainly *i.e.* 30-50° due NE, except and south of Rangpo where dips changes from 30-50° due SE. Tight isoclinal F_2 folds in Lingtse gneisses show intense flattening along the plane of S_2 foliation. The signatures of post-metamorphic thrusting are evidenced in the field by strong retrograde metamorphic effects (chloritization) after the F_3 folding movements (Dubey, 1993).

Petrography

The relationship between S-surfaces, phases of folding and recrystallisation of mineral assemblages were establishied by several workers (Zwart, 1960, 1962; Vernon and Flood, 1979; Johnson, 1990; Bell and Johnson, 1992). On the basis of above works Table 1 correlates growth of various minerals in relation to deformation and metamorphism in metapelites on the basis of detailed petrographic studies in the area.

MINERAL CHEMISTRY

Analytical Techniques

Electron microprobe data of polished thin sections of key minerals in the samples were obtained by electron probe microanalyser (EPMA) and scanning electron microscope (SEM) at Roorkee University. For this purpose, standard operating conditions were 15-20KV accelerating potential, 15 nA specimen current, 15-200 sec counting time, following the method of Bence and Albee (1968) and the correction factors of Albee and Ray (1970). Reproducibility of data is within 1 to 2% for major and minor elements.

Metapelites

Table 2 gives average representative chemical analysis of each of the minerals though a large number of point analyses have been obtained in different metamorphic grades.

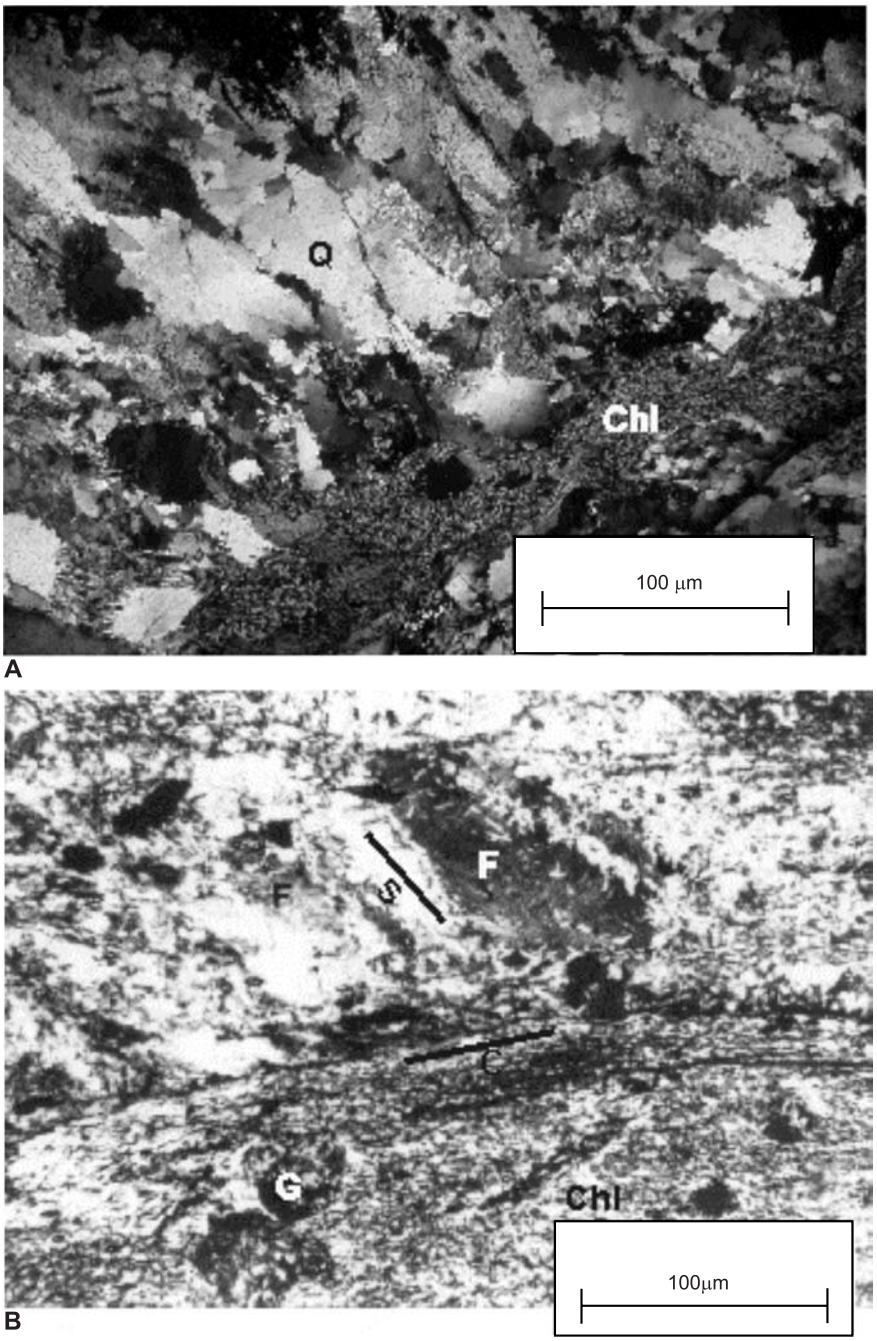

Fig. 2 (A) Photomicrographs showing altered chlorite (peninnine) with obliquely elongated sheared quartz veins in calc-quartzites. (B) Photomicrograph showing sheared contact between Lingtse gneiss and garnet chlorite-schists. The feldspar porphoblast as well as the quartzose and micaceous layers show S – fabric bounded by strong C – plane.

Table 1: *Mineral growth in relation to deformation and metamorphism in Sikkim, Eastern Himalaya.*

	M_1 (Prograde) S_1-S_2	M_{1a} (Retrograde) S_2	M_2 (Prograde) S_2-S_3	M_{2a} (Retrograde) S_3-S_4
Pelites				
Quartz	–	-	–	-
Plagioclase	–	Sericitization Zone	–	Sericitization and epidote formation
Chlorite	–	–	–	Penninine
Chloritoid	–	–	–	–
Biotite	–	Chlorite and Sigmoidal shapes	–	Chlorite
Muscovite	–	Sericite	–	Sericite
Garnet	– (Normal growth zoning)	Chloritization (inverse zoning)	Zoned garnet with inclusion free rims (normal growth zoning)	Chloritization (Penninine) and Chlorite pseudomorphs (reverse zoning)
Staurolite	– (Zn-rich)	Sericitization (decrease in Zn)	Zoned garnet inclusion free Staurolite (increase in Zn)	Sericitization (decrease in Zn)
Kyanite	–	Sericitization/ pyrophyllitization	–	Kinked and deformed cleavage and pyrophyllitization
Sillimanite	–	–	–	Sericitization
K-feldspar	–	Sericitization	Zoning	Muscovite Replacement
	Isoclinal Tight root folds	Sinistral shearing and less retrogression parallel or little oblique to S_2. Reclined and Isoclinal root- less coeval folds	Porphyroblast over growth and zoning open to tight 1B and 1C type folds	Retrogression phyllotization cross folding micropuckering
	F_1	F_2	F_3	F_{3a}
	D_1		D_2	

Table 2: *Selected representative chemical analysis of metamorphic rocks from Sikkim, Eastern Himalaya (Major trace elements in % and traces in ppm).*

Oxides	1	2	3	4	5	6	7	8	9	10	11	12	13
SiO_2	74.34	68.00	72.12	56.35	53.85	69.95	75.47	78.62	72.87	73.26	70.74	81.46	72.21
Al_2O_3	12.57	15.51	20.11	14.21	14.14	13.25	13.60	12.32	13.20	12.38	14.28	9.46	12.78
Fe_2O_3	4.27	12.89	0.05	10.94	17.07	4.80	3.42	2.70	4.20	5.74	5.21	3.62	7.46
CaO	0.14	0.00	4.57	0.05	0.07	0.17	0.19	0.52	1.02	2.00	1.96	0.00	0.06
MgO	1.05	0.00	0.82	9.07	5.40	0.63	1.46	0.75	0.78	0.50	0.89	1.20	1.36
MnO	1.07	0.20	0.08	0.14	0.25	0.09	0.02	0.06	0.06	0.10	0.08	0.07	0.09
K_2O	1.51	1.14	0.42	6.37	3.72	6.56	5.50	1.99	4.17	2.15	3.40	1.03	2.87
Na_2O	3.90	0.54	0.59	1.92	1.74	2.29	1.58	3.14	2.67	3.13	3.23	2.04	1.82
P_2O_5	0.11	0.57	0.91	0.03	0.36	0.09	0.09	0.68	0.66	0.22	0.61	0.76	0.60
TiO_2	0.53	0.58	0.29	0.86	0.70	0.67	0.98	0.25	0.38	0.52	0.48	0.36	0.74
Total	98.49	99.95	99.96	99.94	97.30	100.50	102.31	101.03	100.01	100.00	100.88	100.00	99.99
Fe^{+3}	3.56	11.74	3.73	7.95	17.15	5.64	3.46	2.40	3.85	4.74	4.69	3.12	5.54
Ni	29.62	68.93	15.15	68.93	82.81	31.88	46.89	8.30	19.22	14.91	11.12	14.55	17.77
Cu	15.68	45.86	9.70	45.86	137.50	33.53	30.16	00.00	2.11	33.30	1.78	13.53	25.02
Zn	45.66	13.62	5.35	138.62	138.45	55.21	44.74	27.23	46.64	55.91	60.02	8.37	29.35
Ga	17.48	17.48	17.01	17.48	19.44	22.44	20.48	15.94	16.21	16.67	16.68	16.62	17.91
Pb	21.46	2.75	28.04	2.75	26.60	41.17	36.71	28.02	23.44	27.31	24.85	32.95	25.48
Th	0.71	11.76	18.43	11.76	15.43	19.78	10.41	17.81	13.13	4.88	18.07	19.47	0.00
Rb	93.39	38.25	30.87	205.38	195.45	225.98	172.03	63.64	91.05	180.27	262.68	63.22	167.82
U	0.80	2.85	8.11	7.06	6.04	7.06	5.47	46.38	53.66	7.82	17.14	5.22	0.70
Sr	208.87	N.D	28.62	42.00	52.00	N.D.	35.61	57.38	60.33	87.36	87.03	12.78	21.81
Zr	236.5	356.97	205.48	15.25	15.72	68.28	34.81	81.52	82.14	83.01	50.58	193.80	270.19
Nb	8.92	13.29	1.60	18.92	N.D.	24.12	19.22	78.01	75.59	6.59	10.70	20.09	6.92
Y	20.40	55.07	4.46	N.D.	N.D.	N.D.	N.D.	65.00	68.00	16.61	20.98	29.75	28.93

1. Phyllite Schist; 2. Chloritoid Schist; 3. Garnet Schist;4. Staurolite Garnet Schist;5. Staurolite Garnet Schist; 6. Garnet Schist; 7. Kyanite Sillimanite Schist; 8. Migmatite;9. Migmatite;10. Feld. Gneiss;11. Feld. Gneiss; 12. Lingtse Gneiss; Lingtse Gneiss.

Chlorite: The chlorite in low grade metamorphic rocks of Sikkim is ripidolite and is rich in iron and deficient in magnesium. It is enriched in Al_2O_3. The chlorite from garnet to staurolite zone varies from brunsvigite to pycnochlorite. The Fe/(Fe+Mg) ratio of chlorite in metapelites is usually in the range of 0.2-0.8 (Albee, 1962). The Fe/(Fe+Mg) ratio decreases from chloritoid to staurolite bearing rocks in which the FeO decreases but MgO increases with increasing metamorphic grades. The chloritoid bearing schist shows abundance of alumina and iron oxide as is observed in the chlorite of low grade rocks. The (Al/(Al+Fe+Mg) versus Mg/(Mg+Fe) ratio (Laird, 1989) shows an inverse trend *i.e.* decrease of the ratio in increasing grade of metamorphism.

Chloritoid: Chloritoid is rich in aluminium and iron and shows normal chemical zoning. The abundance of (ferrous) iron, aluminium and low magnesium is a function of the bulk

chemistry of chloritoid bearing schist. The recalculated analysis shows that chloritoid contains very little ferric iron. It shows negligible substitution of Al^{3+} by Fe^{3+} and Fe^{2+} by Mn. Na_2O and CaO also occur in negligible amounts.

Muscovite: The inferred percentage of muscovites (88-94% Mu) from Sikkim contains high K_2O (8.45-9.53), Al_2O_3 (33.33-34.5) while FeO (1.21-2.52), MgO (0.2-0.81) and Na_2O (0.97-1.75) are present in low percentage. These rocks show limited solid solution with paragonite (6-12% pa). The paragonite content increases in chloritoid to staurolite zones and decreases in Kyanite-sillimanite zone. The highest sodium content is in staurolite zone. The increase in Ti content of muscovite is commonly inconsistent with the progressive increase of metamorphism upto staurolite grade (Guidotti, 1974). Al^{iv} content also show an increase from garnet to kyanite-sillimanite grade as observed by Das (1987) in Kishtwar area (Kashmir Himalayas).

Na substitutes for K upto 0.13-0.21 Na/(Na+K) in chloritoid and garnet zones. This content is upto 0.24Na/(Na+K) in the staurolite zone. However the substitution decreases in (0.22 Na/Na+K) kyanite-sillimanite grade samples. The Na-content of muscovite is relatively higher in most of muscovites rich samples which may be due to muscovite co-existing with plagioclase (*cf.* Guidotti, 1969). The maximum amount of Si observed is 3.11/formula in garnet zone whereas it is about 3.09/formula in staurolite and Kyanite-sillimanite zone. According to Labotka (1980) and Hyndman (1985), the phengitic component decreases and is substituted by Na with increasing metamorphic grade. However, in the staurolite zone significantly higher substitution of sodium content is noticed. According to Hyndman (1985) there is a lowering of Si, Fe^{2+} with increasing trend of metamorphic grade. In Sikkim area, Si, Ti, Mg, Na and EY in muscovite show an increase in slope from chloritoid to garnet grade zone while Al^{iv}, Al^{vi}, Fe,K and EX are characterised by a decreasing slope trend. This variation in staurolite and kyanite-sillimanite zone is different than the other rocks, except for a decrease of Al^{vi},and an increase in Mg from chloritoid to kyanite-sillimanite zone. The decrease in Si content from garnet to staurolite zones is due to the effects of shearing and retrogression associated with staurolite zone (*cf.* Goff & Ballevre,1990).

Biotite: The chemical variations in biotite during prograde metamorphism has been worked out by Dhana Raju *et al.* (1977), Ruiz *et al.* (1978), Labotka (1980), Schreurs (1985), Das (1987), Guidotti (1984) and Guidotti *et al.* (1988). The variations of Mg/Mg+Fe, Na/Na+K and Mn content largely depends on the various temperature controlled mineralogical reactions. Ti-content, EXII sites and EVI sites happen to be crystallochemically controlled responses to the variations caused by the metamorphic reactions (Guidotti *et al.*, 1988).

The chemical composition of biotite from Sikkim depicts Mg/Mg+Fe ratios as 0.48-0.49 in garnet zone; 0.49 to 0.53 in staurolite and 0.49-0.50 in kyanite-sillimanite zone respectively indicating the ratio being sensitive to an increasing trend of metamorphism from garnet to staurolite zone. It is consistent with the Mg/Mg+Fe ratio of chlorite for the above zones. The variation of Mg/Mg+Fe of biotite in these zones reflect that with the rise of temperature, the continuous reactions moved the assemblages in more Mg-rich positions field (Guidotti *et al.*, 1988). However, once the assemblages Al_2SiO_5+ staurolite + Biotite + garnet were formed, the continuous reactions made the phase to be more FeO rich in composition (Chinner, 1965). Similar feature is noticed in the Fe-rich biotite (lower Mg/Mg+Fe ratio) from kyanite-sillimanite zone of Sikkim.

In Sikkim area also the Na/Na+K ratio in biotite showed an increase from 0.03-0.04. to 0.082-0.091 in garnet and staurolite zone respectively. It decreased from 0.067 to 0.082 in kyanite-sillimanite zone. This relation was quite consistent in staurolite and kyanite-sillimanite bearing assemblages when the host rock was depleted in Na_2O and MgO (Dubey,1993).

In Sikkim area an increase in Al^{iv}, Mg/Mg+Fe contents is observed with increasing grade of metamorphism whereas Al^{vi}, Ti, Si^{iv}, Na/Na+K and Mn showed a marked decrease in higher grade metamorphites (after Ruiz *et al.* 1978). Guidotti (1984) is of the view that the increase in Ti content with metamorphic grade could be ascribed to biotite saturated with Ti and coexisting with intrinsic Ti phases such as ilmenite and rutile. Thus, Ti content is a function of prevailing intensive parameters. In Sikkim area, the biotite contains ilmenite and the Ti-content biotite (coexisting with garnet) of garnet and staurolite zone is concomitant with increasing metamorphic grade. However biotite of kyanite-sillimanite zone is not saturated with Ti. Dhana Raju *et al.* (1977) noted that the ratio MnOx100 TiO_2 was less than 5.0 (*i.e.*, above 90%) in most of the biotites from high grade rocks (upper amphibolite and granulite facies), whereas it was more than 5.00 in low to medium grade rocks (epidote-amphibolite and greenschist facies). On the basis of above it can be inferred that the rocks of garnet, staurolite and kyanite-sillimanite zones show a transition from epidote-amphibolite to upper amphibolite facies on the basis of MnO versus TiO_2 ratio (*cf.* Dhana Raju *et al.*, 1977). Biotite show increase in Al^{iv} and decrease in Ti in medium to high grade metamorphic rocks (staurolite to kyanite-sillimanite). A marked decrease in MnO in biotite present in negligible amount in higher grades can be related with depletion of MnO in garnet of different metamorphic grades.

Plagioclase*:* The composition of plagioclase is in the range of An_{14-22}. The zoning is common and grain to grain compositional variation is very little and is marked by a decrease of co-existing anorthite content at the rims. The anorthite content of plagioclase increases from staurolite to kyanite-sillimanite zone. As noted by Labotka (1980); the Ca-rich garnet is more akin to co-exist with Ca-rich plagioclase and since these are the only Ca-phases present, the Ca-content is controlled to some extent by the occurrence of Ca in the total rock. In zoned garnet the Ca decreases from core to rim in all the metamorphic zones in Sikkim.

Garnet: Garnet from different metamorphic zones in Sikkim area exhibits a variable distribution of chemical elements *viz.* Fe, Mg, Ca and Mn and is characterized by chemical zoning. The zoned garnets are critical indicators of disequilibrium and are significant in application of increasingly sophisticated models of kinetics of metamorphic processes. The chemical evolution of garnet from Sikkim area is described below :

Garnets from the garnet zone is highly enriched in Mn-core showing a progressive decrease towards rim with a very slight inflection of relatively lower Mn near core. It also exhibits normal growth zoning i.e., Fe+Mg increasing and Ca+Mn decreasing from core to rim (Dempster, 1985). Garnet with normal growth zoning has a grain size varying from 1 to 3mm. The smaller the size of garnets, the larger the volume of rock in which such garnets are formed (Hess, 1971; Dietvorst, 1982). Kinking in the core of such prograde garnet may be due to replacement of chlorite by biotite (Hollister, 1966; Thompson, 1976) overlapping T-X loops. The Mg/Mg+Fe(M/FM) ratio shows a slightly increasing trend varying near the rims (next to biotite) due to the effects of cation diffusion between garnet and biotite rather than any growth or resorption feature, which would mimic the porphyroblast shape

(*cf.* Lasaga *et al.*, 1977). The deficiency of Mn at the rims of the garnet further supports this inference (*cf.* Dempster, 1985). The garnets of this zone contains inclusions of minute chlorite, muscovite and epidote alongwith rutile and $S_i(S_1)$ of quartz and ilmenite in core parts. The S_e in garnet is surrounded by S_2 of syntectonic origin at the rims which are affected by retrogression.

The garnet from staurolite zone shows complex textural and chemical patterns. The garnet is comparatively larger in size than that of the garnet zone (approx. 1- 5mm) and is dotted by clear inclusion-trails in its core which is smaller than inclusion free (ilmenite rich) idioblastic rim and is associated with biotite often showing retrogression.

The core of garnet consists rutile, ilmenite, muscovite and quartz as $S_i(S_1)$ followed by quartz, retrograded chlorite as $S_i(S_2)$ at outer part of core. It is followed by ilmenite and rarely retrogressed biotite near the idioblastic rim. Biotite coexisting with such garnet is mainly of prograde type and shows retrogression at the rims. It is observed that the inner inclusion trail is abruptly truncated in the outerpart of core and often the rim of the garnet is a pseudomorph after chlorite. A few grains show micropuckering or later foliation.

Such type of garnet characterized by an increase of Mn+Ca near the outerpart of core and with a decrease in Mg+Fe show an inverse zoning followed by a normal growth zoning from outer part of core to the inner part of rim. A reverse zoning near the outer part of the rim is also noticed. The inverse zoning *i.e.* enrichment of Mn content from inner core to the outer core is attributed to retrogressive effects (Grant and Weiblen, 1971; De Bethune *et al.*, 1975; Tracy *et al.*, 1976; Tracy, 1982; Dietvorst, 1982; Karabinos, 1984 and Dempster, 1985).

Lal *et al.* (1981) analysing the garnet from Takdah, Darjeeling area suggest that garnet from Zone C (Staurolite-biotite zone) is feebly zoned and is free from inclusions and lacks rotational synkinematic core. It was presumably formed during the post-kinematic phase, between the D_1 and D_2 deformation through a discontinuous reaction. Mohan et al. (1989) observe that Ca-increases from the core and then decreases towards the rim. The changes in garnet growth as suggested by them are in agreement with Crawford (1974) due to the garnet producing reactions. The garnet growth has also been attributed with contemporaneous increasing temperatures (Cygan and Lasaga, 1982). Continuous smooth zoning profiles and lack of textural zones in most of the grains of garnet was explained by them due to uninterrupted garnet growth in a single metamorphic event.

Some of the garnets from staurolite zone lacks distinct textural zones or inclusion free variety is post-kinematic and later possibly grew simultaneous to the overgrown inclusion-free rims. The reversal of chemical zoning *i.e.*, an enrichment of Mn near the rim, has been discussed by several workers because of cation exchange between adjacent garnet and biotite (Hess, 1971; Tracy *et al.*, 1976; Robinson *et al.*, 1977; Lasaga *et al.*, 1977); resorption and reincorporation of Mn into the remaining garnet (De Bethune *et al.*, 1975; Kerr, 1981) and growth by continuous Fe-Mg-Mn exchange reactions between garnet and biotite (Tracy *et al.*, 1976; Thompson, 1976). The biotite inclusions near the rim of garnet show retrogression. Therefore, enrichment of Mn near the rim is due to another retrograde metamorphic event, which equilibrated rapidly with the co-existing minerals. The garnet from staurolite zone is marked by textural unconformities with varied chemical zoning due to multiple tectonometamorphic events and polymetamorphism (Thompson *et al.*, 1977).

The garnet in kyanite-sillimanite zone is coarser in size, varying from 2-7 mm. texturally, some garnet contains inclusions while other are devoid of inclusions. The chemical analysis

of these garnets supports the fact that the content of Mn increases with a decrease in Ca near the rim. Garnet shows an increasing trend of M/FM ratio from Darjeeling-Sikkim (Lal *et al.*, 1981; Mohan *et al.*, 1989). They interpreted the normal growth zoning with a reversed zoning near the rims of garnet due to resorption through a continuous prograde reaction. The zoning pattern of Ca in high grade metamorphic rocks, is complex and reflects the involvement of some calcic phases (*viz.* plagioclase in garnet producing reactions).

The garnet examined from kyanite-sillimanite zone shows no evidence of zoning in its interior parts as observed in garnet from low to medium grade metamorphics. The texture of most grains of garnet (high grade) reveals that it grew under peak metamorphic conditions. As a corollary of the preceding, complete recrystallisation of garnet of lower grade under high grade conditions possibly obliterated the evidences of low grade zoning.

All these types of garnet in the Sikkim depict an increasing M/FM ratio at rims sympathetic to other Fe-Mg phases and a rough trend of decreasing concentrations of Mn is exhibited in the garnet core with increasing metamorphic grades upto staurolite zone and occasionally, in kyanite-sillimanite zone.

Staurolite: The staurolite has been chemically analysed from staurolite and kyanite-sillimanite zones. The staurolite from these zones shows small content of Zn which increases progressively with metamorphic grade. Chemical zoning shows a slightly higher amount of X_{Mg} towards rim (Mohan *et al.*, 1989). Lal *et al.* (1981) described that X_{Mg} in staurolite increased from zone C (Staurolite-biotite) to D (Kyanite-biotite) and decreased from zone D to E (Sillimanite-biotite) and in respect of core and rim parts of staurolite there was a general decrease of X_{Mg}. The progressive increase of Zn-content was attributed to its resorption by the continuous (Fe-Mg-Zn) reaction ($T_{Zn} > T_{Fe} > T_{Mg}$). A progressive increase in Zn-content has also been noticed in staurolite with increasing metamorphic grade of Sikkim. The zoning is clearly related to retrogression of white mica shimmer aggregates (Zn-rich) formed by breakdown of staurolite which was incorporated in remaining staurolite and formed Zn rich mid rim/outer core (similar to retrograde Mn of the garnet). The staurolite in this zone showed a decreasing trend of Ti and Zn at the rim. Al and Fe showed an increase at the rims (Al and Fe being maximum in mid rim/outer core). Mg decreased at the rim but was of increasing order at mid rim/outer core. The M/FM ratio decreased at the rim of staurolite. The appearance of such staurolites showing increase in Zn and low M/FM at the mid rim/outer core parts were possibly formed at the rims of first formed garnets with increasing grade of metamorphism. Such features were more commonly observed in the medium grade rocks where late deformations were accompanied by increasing hydrous retrogression (Dempster, 1985). The presence of staurolite with in staurolite in the medium grade rocks can be ascribed to its multistage growth.

The staurolite in kyanite-sillimanite zone is less abundant and shows a lower M/FM ratio as compared to the previously formed staurolite in staurolites zone. This staurolite shows a slightly high Zn-content from that of the previously formed staurolite. The increase in Zn content in higher grade metamorphic rocks can be explained due to decrease in modal staurolite characterized by staurolite consuming prograde reactions. This staurolite is richer in Fe than that from staurolite zone.

Metamorphism

The rocks of Sikkim area exhibit an inverted sequence of metamorphism. As a result, the grade of metamorphism increases from south to north specially northwards of the M.C.T.

The low grade Daling Formation is overlain by medium to high grade Darjeeling Formation. The prograde metamorphic rocks of the first event (M_1) consist low to high grade metamorphites from greenschists to upper amphibolite facies. The first appearance of chlorite porphyroblast is noticed in the chlorite schist belonging to Daling formation (low grade). This pelitic rock shows a two phase assemblage of muscovite-chlorite. As the bulk rock composition (Dubey, 1993, *cf*. Table 2) shows very high alumina, the increase of modal chlorite (rich in Al_2O_3) is suggestive of the fact that chlorite was formed by the following reaction:

$$\text{Pyrophyllite} = \text{Chlorite} + \text{Quartz} \quad \ldots(1)$$

or

$$\text{Kaolinite} = \text{Chlorite} + \text{Quartz} \quad \ldots(2)$$

Guidotti (1984) observed that rotation of the lines on AFM implies the exchange reaction:

$$\text{Caledonitic Muscovite} + \text{Al-rich Chlorite} = \text{Less Caledonitic Muscovite} + \text{Al-poor Chlorite} \quad \ldots(3)$$

Miyashiro and Shido (1985) described the extent of Tschermark substitution (Mg, Fe) Si= Al_2 in chlorite, muscovite and biotite in low to medium, grade metapelites. They observed that distribution co-efficients of exchange reaction for Tschermak substitution between muscovite and chlorite varied greatly not only with temperature but also with the substitution of the two minerals because of their deviation from their ideal exchange equilibrium, not sensitive to pressure. The caledonite content of muscovite decreased with an increase in temperature.

The chloritoid bearing metamorphic assemblages show the presence of relatively caledonite deficient muscovite, aluminium rich Fe-chlorite *i.e.*, Fe-ripidolite and Fe-chloritoid with magnetite. Hyndman (1985) observed that chloritoid formed with paragonite at the beginning or within biotite zone *i.e.*,

$$\text{Paragonite} + \text{Chlorite} + \text{Quartz} = \text{Chloritoid} + \text{Albite} \quad \ldots(4)$$

Based on this reaction, low content of paragonite (9-15%) in muscovite and absence of albite commonly restrict the occurrence of chloritoid. Winkler (1979) opined that chloritoid persisted throughout the range of low grade metamorphism. The chlorite-chloritoid pair in this assemblage shows a consistent Fe-Mg partitioning. The relative thermometry suggests a temperature of 410 to 450°C. According to Frey (1974) the reaction responsible for first appearance of chloritoid is as following:

$$\text{Pyrophyllite+Iron-rich Chlorite} = \text{Chloritoid} + \text{Quartz} + H_2O \quad \ldots(5)$$

Another reaction at slightly higher temperature described by Thompson and Norton (1968) is

$$\text{Haematite} + \text{Iron-rich Chlorite} = \text{Chloritoid} + \text{Magnetite} + \text{Quartz} + H_2O \quad \ldots(6)$$

They suggested it to be a dehydration reaction although on casual examination, it can be easily mistaken for deoxidation reaction. The presence of high alumina and iron oxide in bulk rock composition along with the abundance of magnetite with Fe-chlorite and chloritoid can be explained by reaction(6) which is mainly applicable for the formation of chloritoid in Sikkim. The low grade metamorphic chlorite schists show strong retrogressive effects with formation of penninite and sericite, during the last stage of second retrograde metamorphism. In the chloritoid schists sheaves of white mica with chloritoid and quartz are also present.

The formation of biotite in K-feldspar free metapelites can be explained by the following continuous Fe-Mg reactions :

Phengitic Muscovite + $Chlorite_1$ = less phengitic muscovite + biotite $\pm$ $chlorite_2$ $\pm$ Quartz ...(7)

3 Muscovite + 5 chlorite = Biotite + 4 Al - Chlorite $\pm$ 7 Quartz + H_2O ...(8)

The altered penninite due to shearing of biotite along the S_2 and alteration of biotite into chlorite later than S_2 can be ascribed to retrograde metamorphic effects.

The appearance of garnet in the rocks is first observed towards north of Ranipul. The garnet co-exists with biotite which shows retrogression to chlorite. The rims of the garnet often, partially or completely are surrounded by penninite. The garnet, very rarely, shows unaltered nature alongwith biotite and is associated with chlorite and muscovite in the metamorphic assemblages. Lal et al. (1981), Das (1987) and Saklani (1993) have reported this mineral assemblage in Lesser Himalayan region. According to Thompson and Norton (1968) garnet and biotite in aluminous rocks are formed due to :

Chlorite + Muscovite + Quartz = Almandine + Biotite + H_2O ...(9)

The other reactions responsible for the first appearance of garnet are :

Chlorite + $Biotite_1$ + Quartz = Almandine + $Biotite_2$ + H_2O ...(10)

Winkler (1979).

Chlorite + Muscovite + Epidote = Almandine rich Garnet + Biotite + H_2O ...(11)

Winkler (1979)

The rocks of garnet zone from Sikkim show Mn-rich and Ca-rich garnet-cores while their rims are rich in Fe and Mg. Such a Mn-rich almandine garnet core is formed by the following continuous reaction:

Muscovite + $Chlorite_1$ + Quartz = Almandine Garnet + Biotite + $Chlorite_2$ ...(12)
(Mn-richer) (Mg-richer)

The rocks of the garnet zone, north of Gangtok stadium, exposed close to staurolite zone, consists of garnet in which chlorite, muscovite and epidote occur as inclusions and also in separate phases in the matrix alongwith biotite. It is to be noted that reaction (11) also took place in calcium rich phases. According to Guidotti *et al.* (1988), the sodium enrichment of muscovite in low to medium grade rocks is due to the following continuous reaction:

Fe-Chlorite + Muscovite = Garnet + Mg-richer Biotite
+ Mg-richer chlorite + Na-richer Muscovite + H_2O ...(13)

This reaction explains the enrichment of sodium in muscovite and an increase in Mg-content of chlorite. Miyashiro and Shido (1985) inferred that these reactions with rising temperature caused a decrease in caledonite content in muscovite, chlorite and the phlogopite content in biotite in the low grade metamorphics. In Sikkim, the inferred reactions can be applied for the formation of phyllites, chlorite and chloritoid schists. The presence of a calcium phase in garnets during an early phase of evolution was completely used up to form either plagioclase or grossularite *i.e.*

Epidote + Quartz = Anorthite + Grossular + H_2O ...(14)

(Guidotti, 1974)

The distribution of CaO, dependent on temperature can be explained by the equation as described by Crawford (1974):

High Ca-Garnet + Na-plagioclase + Muscovite + Chlorite
= Low Ca-Garnet + Ca-plagioclase + Biotite ...(15)

Garnet from garnet zone depicts a small kink in the ternary plots. Hollister (1966) attributed this due to a break in garnet-chlorite tie line and a shift from garnet-biotite tie line to the pseudo-binary T-X loop. Other workers (De Bethune *et al.*, 1975; Dempster, 1985) suggested such a kink due to retrograde effects.

The staurolite zone is mainly exposed in the eastern proximity of the thrust wedge of Lingtse formation (Streaky biotite gneiss) near Gangtok. Staurolite is associated with biotite, chlorite, muscovite, garnet and oligoclase. The Mg-rich chlorite and Na-rich muscovite is present in the core of the garnet, as well as in matrix of the staurolite bearing schists.

The core parts of garnet in this zone consist of inclusions of chlorite, muscovite, rutile, ilmenite and quartz. The quartz inclusions (Si) of S_1 style (Stage 2-3 of Bell and Rubenbach 1983) are enveloped by S_2 inclusion trails of (syn..S_2 foliation) in small core followed by the retrograde chlorite pseudomorph after biotite and altered biotite in the outer parts of core from where the inclusion free overgrowth of garnet has taken place. The overgrown garnet rims are larger in size than the relict cores and occasionally, contain ilmenite inclusions near the outer rims. The biotite in the matrix, near the outer rim also shows retrogression to form chlorite. Often, the overgrown rims are prominently chloritised. A few garnet grains present in quartz and mica domains of staurolite garnet schist do not contain any inclusion and are later formed idioblasts. Small idioblasts of staurolite are enclosed as inclusions in coarse and fractured idioblasts of staurolite. The sheaves of coarse biotite with staurolite of later generation show alteration effects such as chloritization. Lal *et al.* (1981) and Mohan *et al.* (1989) described the following discontinuous reaction for the appearance of staurolite:

Chlorite + Muscovite = Staurolite + Garnet + Biotite + H_2O ...(16)

The garnets described above with a core consisting of inclusions of S_1 and S_2 were followed by the presence of retrograde chlorite in the outer core along with an inclusion free rim, depicting an inverse zoning with Mn-poor and Mg-rich core are followed by an increase of Mn and decrease of Mg-content in the outer part of the core where retrograde pseudomorphs of chlorite after biotite are present. Such cores are overgrown by normal growth zoned rims decreasing in Mn-content and increasing in Mg from the outer part of the core towards the inner part of rim. The inner part of outer rim again shows a reverse zoning followed by normal growth zoning. The low Mn-content and high Mg-content of inner core of garnet and the presence of inclusions of chlorite and muscovite suggests the first appearance of staurolite due to the following continuous reaction:

Chlorite + Muscovite = Staurolite + Garnet + Mg-rich Biotite
+ Mg-rich chlorite + Na-Muscovite + H_2O ...(17)
Guidotti (1974)

The appearance of altered biotite and chlorite in the outer parts of core; an increase of Mn and decrease of Mg; increase of Zn-content in the mid rim/outer core parts of staurolite, are due to retrograde metamorphic effects. This stage possibly enriched the fluids which might have played an important part in the formation of Mn-rich garnet by resorption or due to a continuous reverse reaction.

The presence of overgrown rim showing normal growth zoning over earlier formed core of garnet and inclusion of ilmenite in the outer rim part, presence of staurolite in staurolite; increase of modal biotite and its coarsening to sheaf like biotite flakes, indicate that the retrograde metamorphic stage was stabilized at a faster rate and another prograde metamorphic event formed garnets showing normal growth zoning. Later, coarser idioblasts of staurolite were formed. The staurolite of this generation also shows an increase in Zn content at its rims. The normal growth zoning of garnet rims were consistent with the predicted trend of garnet compositions involved in continuous Fe-Mg-Mn reaction with increasing temperature (cf. Thompson, 1976).

$$\text{Staurolite + Biotite + Quartz = Muscovite + Garnet + } H_2O \quad \ldots(18)$$

Lal *et al.* (1981) and Mohan *et al.* (1989) described reaction (18) for the garnets of staurolite zone in Sikkim-Darjeeling area, and probably studied the later formed normal growth zoned garnets from the staurolite zone. The later formed staurolite and garnet without inclusions are also partially or prominently altered to sericite and chlorite. A few overgrown rims of garnet also show alteration product (penninite-chlorite) and the rock is strongly phyllonitized. The biotite shows alteration into chlorite. Such garnets with postectonically recrystallized partial pseudomorph of chlorite after garnet are enveloped by cross-micropuckers. This implies that the later prograde metamorphic event again culminated in a second retrograde metamorphic event. The garnet from staurolite zone show a reversal of zoning near its outer margin. The increase of Mn and decrease of Mg-content in this zone, suggests resorption or effects of later retrograde metamorphic episode.

Kyanite is first observed associated with biotite and quartz along with staurolite, chlorite and muscovite. Lal *et al.* (1981) concluded that staurolite-chlorite join of staurolite zone is replaced by kyanite-biotite join. Mohan *et al.* (1989) did not observe a direct textural evidence that kyanite grew at the expense of staurolite and muscovite. However, an assemblage consisting of abundant staurolite and muscovite with lesser amount of chlorite and kyanite and plagioclase was followed by abundant kyanite, biotite and quartz in rocks exposed at Dikchu road. Lal *et al.* (1981) suggested a discontinuous (Fe-Mg) reaction mentioned below:

$$\text{Staurolite + Chlorite + Muscovite = Kyanite + Biotite + Quartz} \quad \ldots(19)$$

The Kyanite in the kyanite-staurolite bearing rock shows strong retrogression in which kyanite grains (parallel to S_2) are bent, broken and altered to pyrophyllite. Staurolite alters into sericite and biotite into chlorite. The presence of plagioclase alongwith kyanite in these schists, in significant modal amount, is attributed to a continuous reaction A-Na-K system as described by Lal *et al.* (1981):

$$\text{Na-rich Muscovite + Quartz = Kyanite + Albite + K-rich Muscovite + } H_2O \quad \ldots(20)$$

However, a better discontinuous reaction proposed by Guidotti (1984) can be applied for the mentioned mineral assemblage, on the basis of petrographic observations:

$$\text{Staurolite + Mg-chlorite + Na-Muscovite = } Al_2SiO_5 \text{ (Kyanite)} + \text{Biotite+K-rich Muscovite + Albite + quartz + } H_2O \quad \ldots(21)$$

In most of the metamorphic assemblages the prograde chlorite becomes negligible and so it can be inferred that the reaction (20) possibly continued to increase the modal biotite and kyanite in the late stages due to the following reaction (Mohan *et al.*, 1989):

$$\text{Staurolite + Na-Muscovite + Quartz = Kyanite + Biotite + } H_2O \quad ...(22)$$

A few biotite laths in these gneissic rocks show alteration into chlorite of later metamorphic phase. Plagioclase in these gneissic rocks is more Ca-rich and K-feldspar shows perthitic intergrowth. So, the continuous reaction (21) consisting of Ca-bearing phases continued in the higher grade metamorphic rocks (Guidotti, 1984) :

$$\text{Muscovite + Plagioclase + Quartz = } Al_2SiO_5 \text{ + Na bearing K-Feldspar} + \text{Ca-rich Olgioclase + } H_2O \quad ...(23)$$

In the kyanite-sillimanite zone, the assemblages consisting of garnet, alongwith kyanite, biotite with a decrease of modal muscovite and staurolite, were aided by the kyanite and/or sillimanite; decrease in M/FM ratio of biotite and staurolite; increase in Zn-content of Fe-rich staurolite; K-richer muscovite, Ca-rich plagioclase and zoned K-feldspar. The reaction attributing to the increase in modal amount of kyanite and biotite alongwith garnet as an extra phase has been discussed by Dempster (1985). He observed that an increase in content of Zn in staurolite possibly acted as an internal buffer to the kyanite forming reaction (22). Hence, the staurolite breakdown reaction

$$\text{Staurolite + Na-Muscovite + Quartz = Kyanite + Biotite + Garnet + } H_2O \quad ...(24)$$

(Dempster, 1985)

(24) was important *i.e.*, for the production of kyanite and garnet in the retrograde zones. The alteration of staurolite during the reaction (21) or (22) might have produced garnet in the prograde kyanite-biotite assemblage due to the first retrograde metamorphic stage. It is observed that garnet present in kyanite-sillimanite bearing schists often occurs in broken pieces recrystallised in granoblastic polygonal to platy quartz in the prograde assemblages. The co-existence of kyanite and sillimanite in the higher grade metamorphic rocks can be attributed to the polyphase transformation as exemplified by Carmichael (1969):

$$\text{Kyanite = Sillimanite} \quad ...(25)$$

Banerjee and Bhattacharya (1981) inferred this reaction as a result of breakdown of garnet and staurolite bearing assemblages, instead of the breakdown of muscovite in the presence of quartz. The occurrence of sillimanite alongwith kyanite and increase in modal amount of Fe-rich biotite and increase in Mn, Fe of garnet, K-rich muscovite can also be interpreted by the following continuous reaction (Guidotti, 1974):

$$\text{Mg-Biotite + Muscovite + Garnet + Mg-Staurolite + Quartz = Sillimanite} + \text{Fe-rich biotite + Fe-rich staurolite + Mn-Fe Garnet + Albite + } H_2O \quad ...(26)$$

The presence of Ca-rich plagioclase and zoned K-feldspar point towards the continuous reaction (23) which can be applicable to this zone.

The occurrence of chlorite formed due to alteration of biotite and epidote suggests for the extent of another retrograde metamorphism in the area. Biotite readily alters to chlorite at low to moderate temperatures. Eggleton and Banfield (1985) have mentioned the following coupled reaction for chloritization at 340°C:

$$1 \text{ Biotite + } 0.21 \text{ Anorthite + } 1.64\ H_2O + 1.46\ H^+ \ 0.08\ O_2 = 0.46 \text{ Chlorite + } 0.11 \text{ titanite} + 0.10 \text{ Epidote + } 0.56 \text{ Muscovite + } 0.63 \text{ Quartz + } 0.02 \text{ Magnetite + } 1.46K^+ \quad ...(27)$$

The K^+ released from biotite, sericitized plagioclase and the calcium released from the plagioclase was used to produce epidote and titanite combined with sheet silicates. The presence of sericite requires the addition of water and K^+ and it possibly existed during the

chloritization of biotite. This K^+ also reacted with anorthite component of plagioclase to free Ca^{2+}. It is observed that in vigorous hydrothermal systems, there can be a general flux of ions so that intense secricitization is commonly accompanied by K-metasomatism.

Epidote is also formed as an alteration product of Ca-rich plagioclase due to addition of water *i.e.*,

Oligoclase + tschermakite = Epidote + Chlorite + Albite ...(28)
(Liou, 1973)

In the high grade migmatitic zone, the partial melting might have proceeded in a progressive order *i.e.*,

Higher grade regional metamorphic rocks ® Migmatic (Tronjhemitoids) gneisses ®Granitic gneisses ® foliated granites.

The absence of staurolite from the migmatic tronjhemitoids suggest an increase of temperature to about 700°C as inferred by Winkler (1979):

Staurolite + K-feldspar component in melt = Al_2SiO_5 + Garnet + Biotite ...(29)

The anatexis of a muscovite-plagioclase-quartz gneiss was examined by Winkler (1979). At P_{H_2O} = 5 kb and 680°C an anatectic melt begins to form. At this stage, it is observed that muscovite disappears and the melt is enriched by K-feldspar component. This component, together with albite, quartz and a small amount of anorthite forms a granitic melt. The reaction (23) proposed after Guidotti (1984) in its modified form representing this assemblage is as follows:

Muscovite + Quartz + Plagioclase = K-feldspar + Plagioclase + Quartz component in anatectic melt + An-rich Plagioclase + Sillimanite + H_2O (30)

At higher pressures Fe-biotite in the high grade metamorphic rocks of Sikkim without cordierite, with a slight increase in temperatures, reacted with Al_2SiO_5 (Winkler, 1979):

Biotite + Al_2SiO_5 + 2 Quartz = K-feldspar component + Almandine garnet + H_2O (31)

Sillimanite

Kyanite

and

Biotite + Al_2SiO_5 = Quartz + Albite + Garnet + Melt (32)

Ghose (1979) working on the melting relationship between schists and gneisses of Darjeeling area experimentally noticed the disappearance of muscovite at 715°C-725°C at 7kb with an approximate 30 per cent of melt and the appearance of the new phases of cordierite, ortho-amphibole, ortho-pyroxene and sillimanite at the expense of quartz and biotite in sericite-chlorite schist. The melting of sillimanite gneiss began at 677°C at 5 kb with 5 percent melt and muscovite disappeared between 680°C-700°C. The crystalline phases—biotite, quartz and sillimanite remained stable with 25 per cent rock-melt upto 730°C. Commonly the plagioclase (sodic) gets melted at a few degrees centigrade higher than muscovite in the gneisses.

P-T conditions of metamorphism

Geothermometry: The temperatures have been estimated on the basis of Fe-Mg partitioning in garnet-biotite pairs for medium to high grade assemblages and garnet-phengite for low grade assemblages.

Table 3: *Representative microprobe analyses of minerals from Sikkim metapelites, Eastern Himalaya.*

Mineral	Chlorite			Chloritoid								Muscovite				
Zones	Chloritoid	Garnet	Staurolite	1		2		3		4		Chloritoid		Garnet	Stauro-lite	Kyanite-Sillimanite
				Rim	Core	Rim	Core	Rim	Core	Rim	Core	a	b			
SiO_2	22.62	23.50	25.82	23.53	23.56	24.08	24.19	23.61	23.68	23.47	23.84	44.02	44.81	44.54	45.34	45.18
TiO_2	0.05	0.06	0.14	-	-	-	-	-	-	-	-	0.14	0.17	0.27	0.46	0.38
Al_2O_3	22.10	23.60	22.12	38.90	38.39	39.64	38.34	39.10	38.83	38.43	39.60	33.80	34.52	33.26	34.16	34.11
FeO	35.09	29.40	24.88	25.61	24.06	24.84	24.40	25.22	23.83	24.24	24.70	2.52	1.74	1.11	1.21	1.32
MnO	0.04	0.12	0.06	0.09	0.08	0.16	0.10	0.04	-	0.03	0.02	0.01	0.03	0.07	-	0.02
MgO	5.58	11.60	16.72	1.10	0.85	1.44	1.16	1.83	1.61	1.76	1.76	0.25	0.19	0.72	0.80	0.81
CaO	0.02	-	-	-	-	0.04	0.02	-	-	-	-	0.03	-	0.04	0.05	0.02
Na_2O	-	-	-	0.04	0.02	-	0.02‘	-	-	0.03	-	0.97	1.56	1.51	1.75	1.62
K_2O	0.01	-	-	0.01	0.001	0.006	0.02	-	-	-	-	9.53	8.85	9.14	8.45	8.85
Cr_2O_3	-	-	-	-	-	0.008	0.039	-	0.03	-	-	-	-	-	-	-
NiO	-	-	-	-	-	0.12	-	-	-	0.018	-	-	-	-	-	-
ZnO	-	-	-	-	-	-	-	0.08	-	-	-	0.140	0.01	-	-	0.08
Total	85.49	88.28	89.74	89.37	86.97	90.51	88.35	89.34	88.22	88.05	90.54	94.58	92.24	90.79	92.24	93.05
	Cations based on 28 oxygens			Cations based on 12 oxygens								Cations based on 28 oxygens				
Si	5.18	5.99	6.15	2.02	2.07	2.03	2.10	2.02	2.07	2.05	2.04	6.19	6.16	6.22	6.19	6.18
IV	2.82	2.01	1.85		-							1.81	1.84	1.78	1.81	1.82
Al				3.94	3.97	3.94	3.92	3.98	3.94	3.95	3.95					
VI	3.14	3.29	2.79	-	-	-	-	-	-	-	-	3.69	3.76	3.69	3.68	3.68
Ti	0.01	-	-	-	-	-	-	-	-	-	-	0.01	0.01	0.03	0.05	0.04
Fe	6.72	6.27	4.96	1.84	1.76	1.75	1.76	1.75	1.74	1.76	1.76	0.29	0.20	0.13	0.14	0.15
Mn	0.01	-	0.01	0.006	0.005	0.01	0.007	-	-	-	-	-	-	0.01	-	-
Mg	1.90	4.40	5.94	0.14	0.11	0.18	0.19	0.20	0.18	0.20	0.20	0.05	0.03	0.15	0.16	0.16
Ca	-	-	-	-	-	-	-	-	-	-	-	-	-	-	-	-
Na	-	-	-	0.006	0.003	-	-	-	-	-	-	0.26	0.41	0.41	0.46	0.43
K	-	-	-	-	-	-	-	-	-	-	-	1.71	1.55	1.63	1.47	1.54
Zn	-	-	-	-	-	-	-	-	-	-	-	0.01	-	-	-	0.01
Total	19.78	21.96	21.40	7.95	7.92	7.91	8.00	7.95	7.93	7.96	7.98	14.02	13.96	14.05	13.96	14.11

Contd...

Table 3: *(Contd.)*

Mineral Zone	Garnet								Staurolite								Kyanite-Sillimanite	
	Garnet		Staurolite						Kyanite-Sillimanite					Staurolite			Kyanite-Sillimanite	Kyanite-Sillimanite
	a	b	a	b	c	d	e	f	a	b	c	d	e	Rim	Core	Rim	Core	
SiO_2	35.68	35.20	35.65	36.71	35.20	35.07	34.22	34.91	34.54	34.82	34.45	35.01	34.47	63.61	63.68	62.50	62.36	62.04
TiO_2	1.45	1.38	1.28	1.22	1.31	1.32	1.31	1.30	1.30	1.45	1.68	1.49	1.37	0.04	0.04	0.03	0.04	0.02
Al_2O_3	18.88	18.87	19.08	19.53	18.96	19.30	18.57	18.88	19.33	19.40	19.17	19.78	19.71	21.39	21.96	22.96	22.86	22.80
FeO	18.97	18.98	16.69	18.69	15.85	18.01	16.87	17.87	18.55	17.97	17.43	17.75	17.91	0.07	0.03	0.07	-	0.06
MnO	0.10	0.04	0.07	-	0.04	-	0.05	-	-	0.01	0.01	0.04	0.04	-	-	-	-	-
MgO	9.86	10.41	7.79	10.44	10.42	10.32	9.92	9.93	10.06	10.09	9.71	10.31	10.53	0.00	0.02	0.02	0.01	
CaO	0.03	0.10	0.03	0.05	-	-	0.03	0.05	0.02	0.06	0.05	0.03	0.06	3.08	3.21	4.45	4.51	4.64
Na_2O	0.25	0.21	0.57	0.53	0.53	0.50	0.61	0.54	0.39	0.48	0.49	0.44	0.50	10.63	10.60	9.54	9.14	9.40
K_2O	8.98	8.32	8.35	8.77	8.77	8.61	8.36	8.48	8.31	8.51	8.59	8.59	8.67	0.21	0.14	0.09	0.12	0.08
ZnO	0.06	0.07	0.09	-	-	0.11	0.05	0.05	-	-	0.01	0.12	-	-	-	-	-	-
Total	94.48	93.69	90.85	95.97	91.87	93.39	90.35	92.06	93.53	93.67	91.60	93.57	94.66	99.04	99.68	99.74	99.04	99.06
	Cations based on 22 Oxygens													Cations based on 8 Oxygens				
Si	5.46	5.42	5.46	5.49	5.50	5.40	5.45	5.45	5.37	5.39	5.40	5.37	5.39	2.84	2.83	2.78	2.79	2.78
IV	2.54	2.58	2.54	2.41	2.50	2.60	2.55	2.55	2.63	2.62	2.60	2.64	2.61	-	-	-		
Al														1.13	1.15	1.20	1.20	1.20
VI	0.87	0.84	1.00	1.03	0.99	0.91	0.94	0.92	0.91	0.91	0.86	0.93	0.92					
Ti	0.17	0.16	0.15	0.14	0.15	0.15	0.16	0.15	0.15	0.17	0.20	0.17	0.16	0.00	0.00	0.00	0.00	0.00
Fe	2.43	2.44	2.20	2.34	2.07	2.32	2.25	2.41	2.41	2.32	2.28	2.28	2.28	0.00	0.00	0.00	-	0.00
Mn	0.01	0.00	0.01	0.00	0.00	0.00	0.01	-	-	0.00	0.00	0.00	0.00	-	-	-	-	-
Mg	2.25	2.39	2.30	2.32	2.42	2.37	2.33	2.34	2.34	2.33	2.27	2.35	2.39	0.00	0.00	0.00	0.00	-
Ca	-	0.01	-	0.01	-	-	-	-	-	0.01	0.01	-	0.01	0.15	0.15	0.21	0.22	0.22
Na	0.07	0.06	0.17	0.15	0.16	0.15	0.19	0.12	0.12	0.15	0.15	0.13	0.15	0.92	0.91	0.82	0.79	0.82
K	1.75	1.63	1.68	1.67	1.75	1.69	1.70	1.65	1.65	1.68	1.69	1.68	1.68	0.01	0.01	0.00	0.01	0.00
F	0.07	-	0.22	-	-	0.10	0.36	-	-	0.71	0.07	-	0.30	-	-	-	-	-
Zn	0.01	0.01	0.01	-	-	0.01	0.00	0.00	-	-	0.00	0.01	-	-	-	-	-	-
Total	15.69	15.60	15.76	15.57	15.56	15.72	15.96	15.60	15.59	16.31	15.63	15.58	15.91	5.06	5.05	5.03	5.01	5.03

Contd...

Table 3: *(Contd.)*

	Garnet										Staurolite											Kynanite-Sillaminite	
Mineral Zone	Garnet										Staurolite			Kyanite-Sillimanite		Staurolite		MR/Outer	Kyanite Sillamanite			Kyanite-Sillimanite	Kyanite-Sillimanite
	Rim						Core	Rim			Core	Rim											
	a	b	c	d	e	f	g	a	b	c	d	e	Rim	Core	Rim	Core	Rim	Core	Core	Rim	Core		
SiO_2	36.16	36.04	36.17	36.27	36.46	36.12	36.87	36.47	35.86	36.00	37.85	36.17	36.18	37.03	27.10	27.30	26.79	27.87	26.96	26.98	27.55	37.38	37.67
TiO_2	-	-	-	-	-	-	-	-	-	-	-	-	-	-	0.46	0.49	0.38	0.52	0.64	0.42	0.50	0.00	-
Al_2O_3	20.40	20.55	20.59	20.32	20.67	20.54	20.96	21.01	20.17	2.55	21.32	20.28	20.35	20.42	51.78	50.90	51.46	52.83	50.45	50.77	51.00	16.25	58.80
FeO_2	36.63	36.64	35.69	33.42	34.10	33.36	31.95	35.46	34.69	35.10	32.66	33.48	35.19	34.20	13.19	12.99	11.63	13.10	10.92	13.25	13.37	0.16	0.21
MnO	0.38	1.00	2.30	2.71	2.33	3.69	5.06	0.80	0.57	1.39	2.60	1.51	4.12	3.70	0.16	0.14	0.09	0.10	0.09	0.02	0.08	0.04	-
MgO	2.61	2.33	2.27	2.27	2.55	2.58	1.97	3.43	3.42	2.70	2.47	3.08	0.45	0.29	1.64	1.71	1.56	1.89	1.85	1.76	1.81	0.01	0.04
CaO	2.29	2.30	2.17	2.25	2.38	2.48	2.94	1.54	2.26	2.73	3.08	2.23	2.82	3.61	-	-	-	-	0.01	0.03	0.00	-	0.07
ZnO	-	-	-	-	-	-	-	-	-	-	-	-	-	-	0.16	0.17	0.13	0.16	0.11	0.20	0.25	-	-
Total	98.48	98.87	99.20	97.24	98.50	98.77	99.75	98.68	96.97	98.46	99.99	96.75	99.11	99.25	94.51	93.71	92.05	96.48	91.03	93.43	94.56	98.84	96.79
Cations based on																							
	12 Oxygens													48 Oxygens								20 Oxygens	
Si	2.98	2.96	2.97	3.01	2.99	2.97	2.99	2.97	2.98	2.96	3.03	3.00	2.99	3.03	8.12	8.24	8.17	8.16	8.29	8.18	8.26	4.21	4.19
Al	1.98	1.99	1.99	1.99	1.20	1.99	2.00	2.02	1.97	1.99	2.01	1.98	1.97	1.97	18.29	18.11	18.50	18.24	18.28	18.15	18.01	7.62	7.72
Ti	-	-	-	-	-	-		-	-	-	-	-	-	-	0.10	0.11	0.08	0.11	0.15	0.09	0.11	0.00	0.02
Fe	2.52	2.52	2.45	2.32	2.34	2.29	2.17	2.42	2.41	2.42	2.19	2.32	2.43	2.34	3.31	3.28	2.97	3.21	2.81	3.36	3.35	0.01	-
Mn	0.03	0.07	0.16	0.19	0.16	0.26	0.35	0.05	0.04	0.09	0.17	0.10	0.03	0.02	0.04	0.04	0.02	0.03	0.02	0.01	0.02	-	-
Mg	0.32	0.29	0.28	0.28	0.31	0.32	0.24	0.42	0.42	0.33	0.29	0.38	0.35	0.29	0.73	0.77	0.71	0.82	0.65	0.79	0.81	-	-
Ca	0.20	0.20	0.19	0.20	0.21	0.22	0.25	0.13	0.20	0.24	0.26	0.20	0.25	0.32	-	-	-	-	0.00	0.01	0.00	-	-
Zn	-	-	-	-	-	-	-	-	-	-	-	-	-	-	0.03	0.03	0.03	0.03	0.02	0.04	0.05	-	-
Total	8.03	8.04	8.04	8.00	8.01	8.04	8.01	8.01	8.03	8.03	7.96	8.00	8.02	7.98	30.63	30.59	30.49	30.61	30.42	30.65	30.62	11.84	11.93

Garnet-biotite pairs: As already mentioned, the garnet from garnet and staurolite zone is characterized by normal growth, inverse and reverse zoning. Garnet in the kyanite-sillimanite zone was more homogenised. For the estimation of temperature of garnet-biotite pairs, the models of Ferry and Spear (1978), Hodges and Spear (1982) and Ferry and Spear versus Berman (1990) were applied (Table 3). The temperatures and pressures have been calculated by using a composite computer programme 'Thermobarometry' (Spear and Peacock, 1990) inclusive of a new model Ferry and Spear versus Berman (1990). The author aimed the results by examining the microprobe data of garnet—biotite pairs from different metamorphic zones.

The results obtained by the three models for garnet-biotite pairs from different metamorphic zones are quite consistent. The temperatures estimated lie in range of 490 to 527°C for rim, 465 to 490°C/4-5kb for core of garnet zone; 546 to 575°C for rim, 492 to 522°C for outer core and 555-576°C/5-6kb for core parts of staurolite zone; 658 to 695°C for rim and 630 to 675°C/7-7.5kb for core of kyanite-sillimanite zone, respectively. Neogi *et al.*, 1998; Catlos *et al.*, 2000; Ganguly *et al.*, 2000 have inferred the pressure and temperature for sillimanite-k-feldspar zone (K-feldspar in) in the HHC, Eastern Himalaya ranging from 820°-850°C and pressure 8.8 -11.8 kbs. This higher variation in pressure and temperature in comparison to 658°-770°C temperature and 7-7.5 kbs pressure given by other workers (Mohan *et al.*, 1989 and Dubey, 1993) which is different as the later P-T are in sillimanite-muscovite zone (muscovite in).

Garnet-muscovite pairs: The Fe-Mg ratio between co-existing garnets and phengite were studied by Krogh and Raheim (1978). The thermometer was applied to garnet-phengite pairs from garnet zone of the area and temperatures inferred are 485°C for the core and 510°C for rim-parts of garnet under 4-5Kb. These values are also consistent with the temperatures estimated by Hodges and Spear (1982).

Geobarometry: Different mineral equilibria involving high volume change (V) of the reactions are commonly applied for the estimation of pressure conditions in relation to temperatures inferred by various models of geothermometers. The model given by Newton and Haselton (1981), which is based on reaction (garnet-plagioclase-sillimanite/kyanite-quartz) has been applied to infer the pressure experienced by the kyanite-sillimanite zone in Sikkim.

The most significant limitation of this geobarometer is that the end member equillibrum is known within ± 2Kbrs. The uncertainties are generated by the long extrapolation of pressure and evaluation of grossular activity in garnet solutions at 95% dilution. Thus, a comparative geobarometry based on Ghent and Stout (1981) model was also applied to the kyanite-sillimanite assemblage.

Following the method by Newton and Haselton (1981), the pressure for kyanite-sillimanite zone is estimated as 7-7.2Kb but according to the model of Ghent and Stout (1981) it ranges from 6.9-7.3Kb. These estimates are compatible with one another and are much closer to the estimation of Lal *et al.* (1981). Pressures were also calculated for Staurolite zone by applying the model of Hoisch (1990). It is based on empirical calibration of six different geobarometers for the mineral assemblage:

Quartz + muscovite + biotite + plagioclase + garnet

Based on this geobarometer a pressure of 6.6 to 6.7Kb is inferred for rims and 5.7Kb for the core parts of garnet in staurolite zone. The temperatures and pressures estimates of

Mohan *et al.* (1989) are too high for garnet zone and these in fact correspond to the pressure estimated for staurolite zone of the area. The pressure estimated for this zone is low as revealed by the retrogressed outer core parts of garnet. Figure 3 shows P-T-t paths (arrow), AFM topology and inferred important mineral reactions and assemblages in Sikkim.

GEOCHRONOLOGY

Analytical Procedure

Ion Microprobe Th-Pb dating of monazite has been carried out at UCLA is briefy summarized. 15-25 μm diameter oxygen (O^-) primary beam is used to sputter positive ions from the surface of the sample. The intensity of the primary beam ranges from 2 to 13 nA during different analysis sessions. A mass resolving power of ~5000 is sufficient to separate molecular interferences and distinguish between Pb isotopes in the 204-208 mass range (Harrison *et al.*, 1999). Specially, a 50eV energy window with a 10 to 15eV offset for $^{232}Th^+$ is used. The magnet is steeped through six different mass species: $^{204}Pb^+$, $^{207}Pb^+$, $^{208}Pb^+$, $^{232}Th^+$, ThO_2^+ and U^+. This cycle was repeated 15 times to correct for variations in beam ability and average values were used to calculate ages. Determination of the $^{208}Pb^+/^{232}Th^+$ sensitivity factor is accomplished by dividing the measured magnet $^{208}Pb^+/^{232}Th^+$ value of a standard monazite at a reference $^{208}Pb^+/^{232}Th^+$ value by standard's known daughter to parent ratio. The age of an unknown, measured under identical operating conditions, is determined by applying this sensitivity factor to the measured $^{208}Pb^+/^{232}Th^+$ value of the unknown. The reproducibility of the calibration line is the limiting factor on the precision of ion microprobe age determinations.

All in situ Th-Pb age analyses utilized monazite standard 554, a peraluminous granodiorite from Santa Catalina Mountains in Arizona (Force, 1997). Monazite grains dated in situ are typically analyzed with one spot, limited by the size and irregular shape of the grain (typically <60 μm diameter) and primary beam (typically ~25-30 μm diameter), as well as the optical capabilities of the reflected light microscope attached to the ion microprobe. Two analyses are performed on each spot to identify any variation in age as the ion beam drilled deeper into the grain. Reported ages are corrected from common^{204}Pb using and assumed $^{208}Pb/\ ^{204}Pb = 38.6$ (Stacy and Kramers, 1975). Himalayan monazite grains typically yield >95% radiogenic ^{208}Pb (Catlos, 2000; Gilley, 2001).

Monazite Dating

A detailed geochronological studies and their metamorphic relationship has been described by Catlos *et al.* 2003. Lesser Himalaya samples have garnet + biotite + staurolite + muscovite + plagioclase + chlorite + ilmenite + apatite + monazite + zircon + xenotime + quartz. MCT shear zone rock (CMP860) has garnet + biotite + sillimanite + muscovite + plagioclase + chlorite + ilmenite + monazite + tourmaline + zircon + apatite + allanite + quartz, whereas samples CH14103 have garnet + biotite + staurolite + muscovite + plagioclase + chlorite + ilmenite + zircon + monazite ± xenotime ± apatite ± allanite + quartz. Greater Himalayan Crystallines (Catlos, 2002c). All mineral grains were dated using an ion microprobe and the reader is referred to Catlos *et al.* (2002b) for technical details of in situ Th-Pb ion microprobe monazite analysis, and Schneider *et al.* (1999) for U-Pb ion microprobe dating of zircon. The errors for all ages reported in this paper are 1σ. MCT shear zone rock CMP860 (650±10°C, 6±1 kbar; Fig. 5b, c, d) has monazite inclusions in garnets that range from 20.5±0.6 Ma to 10.8±0.3 Ma (Fig. 5b, c, d). The garnet also contains inclusions of quartz, apatite, allanite,

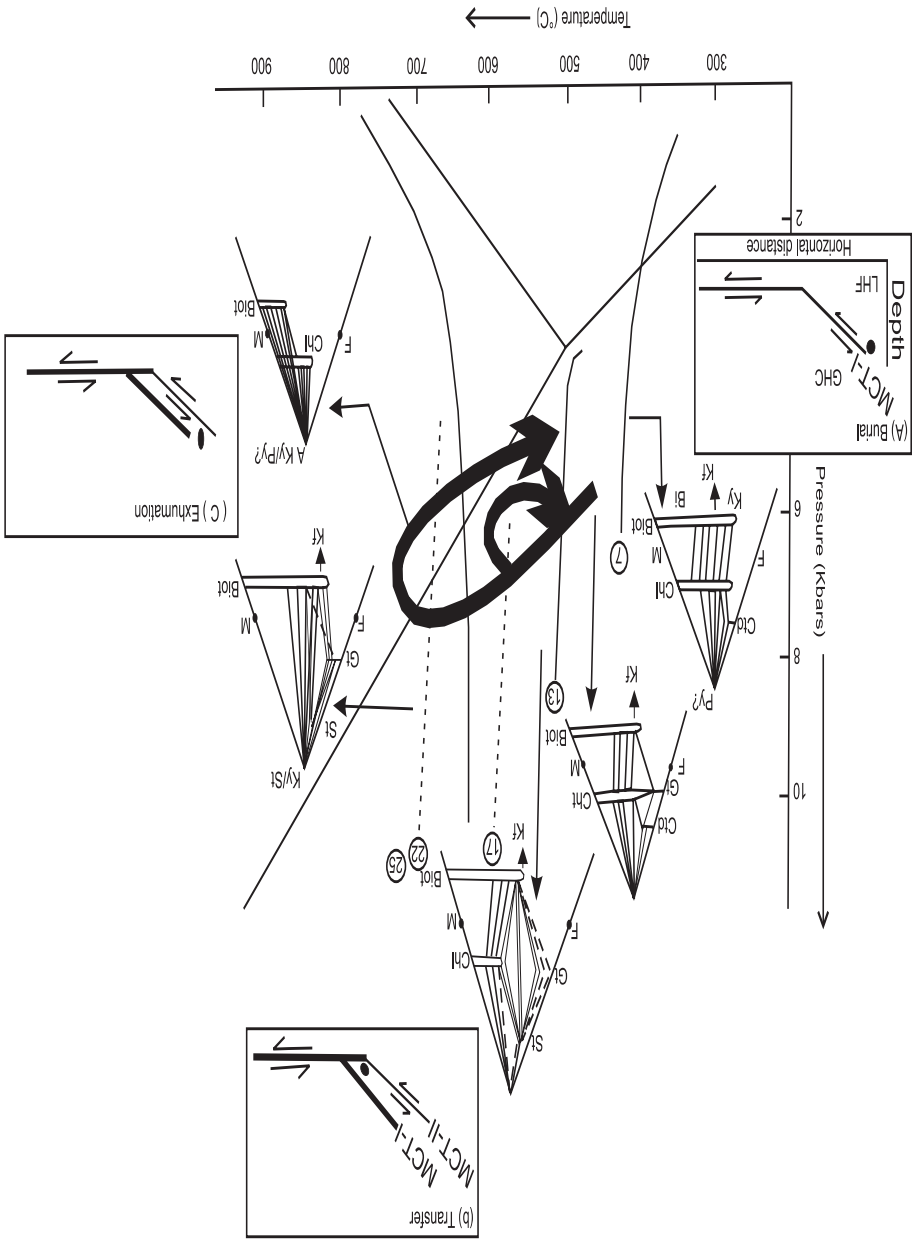

Fig. 3. P-T-t paths (arrow), AFM topology and inferred important mineral reactions and assemblages in Sikkim, Eastern Himalaya.

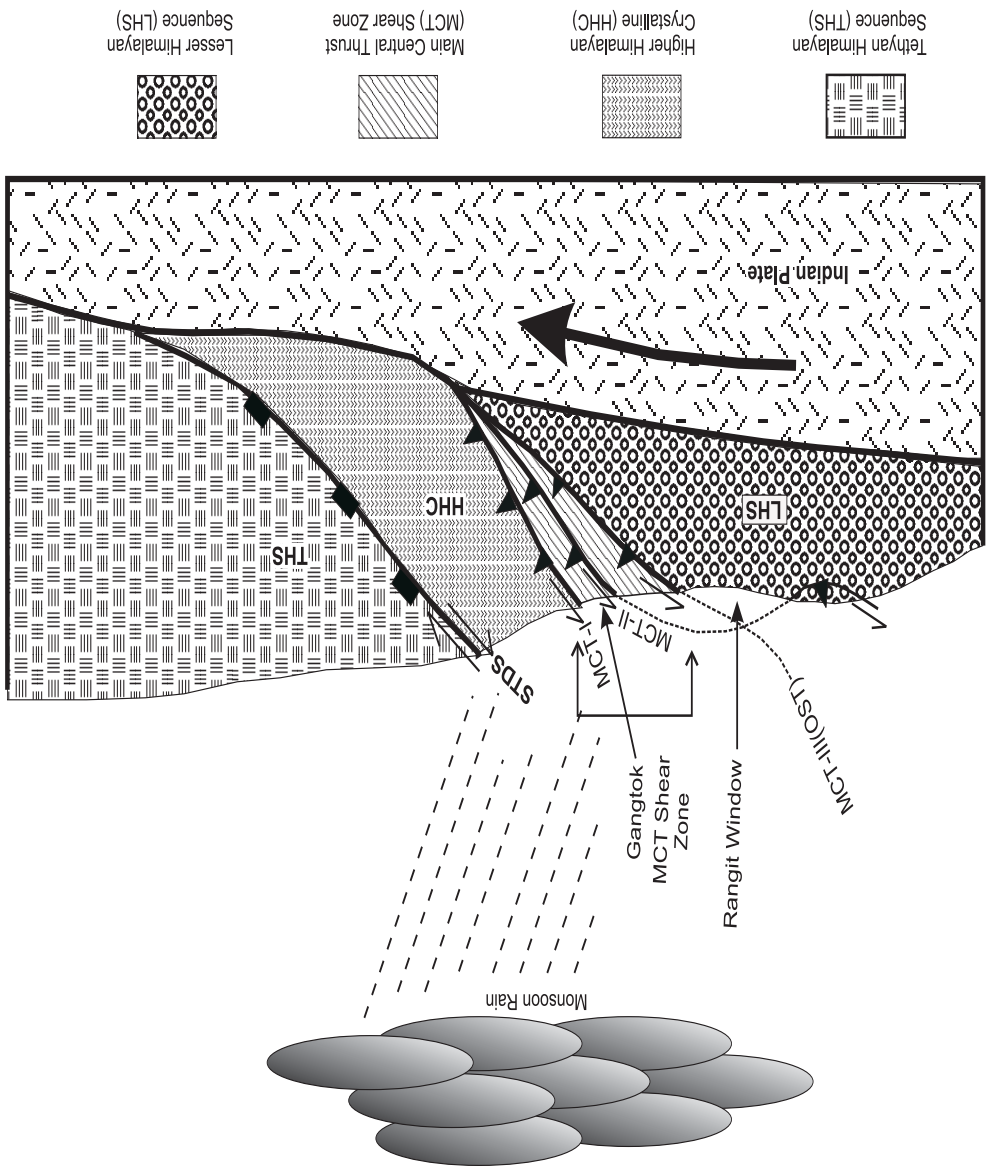

Fig. 4. Schematic cross section showing the positions of MCT-I, MCT-II and OST (MCT-III) in Sikkim, Eastern Himalaya.

monazite, biotite, quartz, and plagioclase and records peak conditions below the closure temperature of Pb in monazite (*e.g.*, Smith & Giletti, 1997). Thus the age distribution in this rock suggests the sample went through a minimum of two monazite forming reactions during the Miocene (~20 Ma) and Late Miocene (14-10 Ma). As inclusions of both ages are found in garnet, a mineral that armors monazite against daughter product loss (*e.g.*, Montel *et al.,* 2000), The garnet is diffusively zoned or experienced retrograde garnet resorption (*e.g.*, Spear, 1991), as seen by the increase at the rim in MnO (~0.05 wt% to 2.8 wt%) and Fe/(Fe+Mg) (from 0.85 to 0.90). However, the garnet displays two broad increases in pyrope from core to rim that appear to roughly mirror decreases in grossular, leading to the irregular compositional traverse and is overall consistent with a change in metamorphic history or mineral assemblage during growth. Further support for our hypothesis that monazite grains in CMP860 record crystallization is given by similar monazite ages found in rocks collected within the MCT shear zone and further south that experienced lower thermal conditions, but similar or higher pressures. For example, sample CHG14103 (525±25°C; 6±1 kbar) has 12-14 Ma inclusions in staurolite (Fig. 5f). The garnet in CHG1403 (Fig. 5f) records growth zoning as evidenced by the bell-shaped pattern of spessartine (from 3 to 0.1 wt% MnO) and overall decrease in Fe/(Fe+Mg) from core to left rim (0.92 to 0.89). The inclusion pattern is curved and continuous with the fabric outside the garnet, suggesting tectonic growth. This garnet has lower grossular and increased pyrope content near its larger quartz inclusions, leading to the irregular zoning pattern from core to right rim (Catlos, 2002a). Note that conditions for estimated for MCT shear zone rocks CMP860 and CHG1403 (Fig. 5b, c, d) are similar to those reported by Lal *et al.* (1981) (560-583°C), Mohan *et al.* (1989) (594-659°C, 5-8 kbar), and Dubey (1993) (546-575°C, 5-6 kbar) and Catlos *et al.* (2003). Lesser Himalaya samples KBP1062A (610±10°C; 7.5±0.5 kbar, Fig. 5a) ~12-13 Ma monazite inclusions in garnet, similar to those analyzed in MCT shear zone rocks.

The following observations could be made moving south through the Greater Himalayan Crystallines, MCT shear zone, and Lesser Himalaya: (1) average monazite ages decrease from Miocene to Late Miocene, (2) garnet grossular patterns change from patchy zoning (CMP860) to relatively flat (CHG1403), (3) garnets appear to begin to preserve growth zoning patterns (CHG14103). We expected thermal conditions change from high (~700°C) to lower temperature (~525°C) moving south through the shear zone, but one Lesser Himalaya sample appears at a higher temperature and potentially higher pressure than the MCT shear zone rock (CHG14103; Fig. 5f).

Modeling of inverted metamorphic sequences in Sikkim

Monazite grains dated in MCT shear zone suggest that the structure was active during the early Miocene (~22 Ma). Harrison *et al.* (1998) estimate that ~20-30 MPa shear heating along the thrust flat that cuts through Indian rocks is capable of producing the leucogranite injection complex. Note that the sample's 4 positions depicted in Fig. 1b are based on the P-T constraints reported in this paper. Thus it could be observed that CMP860 experienced similar baric conditions as the other MCT shear zone sample CHG14103, but higher temperatures (Fig. 5f), probably due to its closer proximity to the hotter hanging wall. This age may be the result of: (1) Pb loss from ~22 Ma grain, (2) a crystallization event related to MCT movement at this time, or (3) a crystallization event not related to MCT movement but facilitated by Miocene emplacement of the Greater Himalayan Crystallines. Thus the rocks experienced conditions not only conducive to monazite growth during Miocene MCT movement,

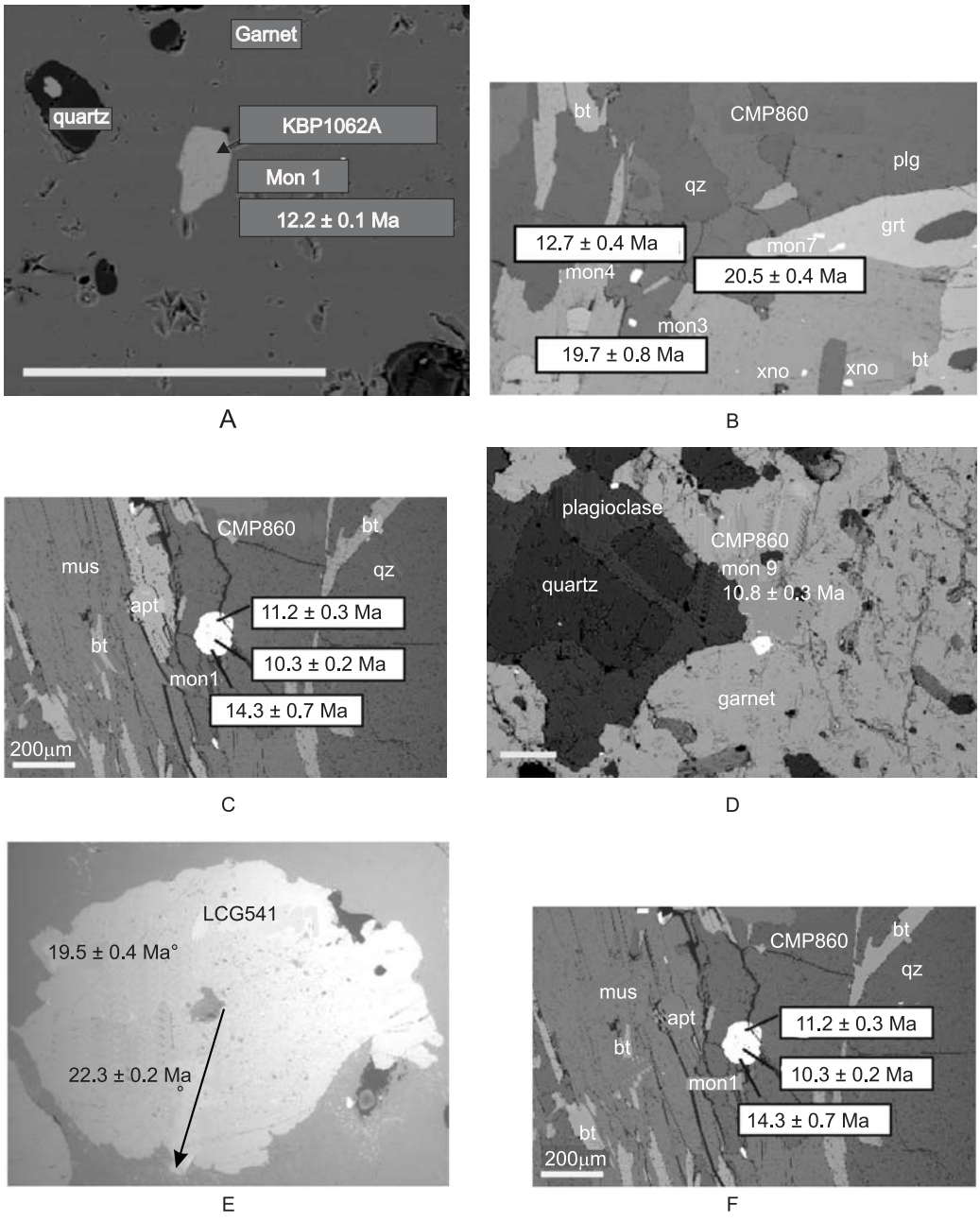

Fig. 5. Ages of Sikkim Himalaya monazite inclusions in Garnet and Staurolite (modified after Catlos *et al.*, 2003)

but also hot enough to experience huge amount of Pb loss. However, garnet crystallized in this rock between 12.2±0.1 Ma and 11.5±0.2 Ma, based on its monazite inclusions of (Table 4), The Lesser Himalaya rock were far from the Greater Himalayan Crystallines, thus would experience crystallization ~4 m.y. after MCT movement. The youngest monazite grains dated

Table 4: *In situ monazite age results from Lesser Himalaya, MCT shear zone and Higher Himalayan Crystalline, Sikkim, Eastern Himalaya.*

Sample[a] (Grain spot)	Monazite location[b]	Age (Ma) (±σ)	ThO_2+/Th+[e] (±σ)	^{208}Pb(%)[d] (±σ)	^{208}Pb*/Th+[e] (±σ)
KBP1062A (Lesser Himalayan Sample)					
10-1[f]	i	12.1(0.6)	3.343 (0.034)	64.9 (2.8)	5.973E-04 (3.084E-05)
KBP1062A Calibration: (0.049±0.002)x+(2.184±0.085); r^2=0.991; ThO_2^+/Th+=3.946±0.276[f]					
CMP860 (MCT shear zone)					
7-1	i	20.5(0.6)	3.411(0.018)	92.1(1.2)	1.015E-03 (2.996E-05)
8-1	m	19.7(0.8)	3.299(0.013)	80.4(2.1)	9.940E-04 (3.385E-05)
4-1	m	12.7(0.4)	3.557(0.019)	84.4(1.8)	6.277E-04 (1.885E-05)
1-2	m	10.3(0.2)	3.800(0.018)	87.5(1.7)	5.117E-04 (1.224E-05)
CMP860 Calibration 1: (0.049±0.001x +(2.184±0.085;r^2=0.991; ThO_2^+Th+=3.946±0.276f[f]					
9-1	i	10.8(0.3)	3.558(0.054)	85.3(1.6)	5.362E-04 (1.359E-05)
CMP860 Calibration 2: (0.099±0.001)x +(0.0881±0.037); r^2=0.948; ThO_2^+/Th+=4.028±0.668[f]					
CHG14103 (MCT shear zone)					
2-1	m	13.8(0.5)	3.328 (0.020)	90.1 (1.1)	6.826E-04 (2.310E-05)
1-1	m	12.9(0.5)	3.380 (0.015)	92.1 (0.9)	6.380E-04 (1.866E-05)
3-1	m	12.2(0.4)	3.556 (0.035)	87.5 (1.3)	6.035E-04 (2.099E-05)
CHG14103 Calibration: (0.049±0.002)x +(2.184±0.085); r^2=0.991; ThO_2^+/Th+=3.946±0.276[f]					
LCG541 (Higher Himalayan Crystalline)					
3-1	i	22.3 (0.2)	3.744 (0.015)	94.4 (0.3)	1.105E-03 (1.108E-05)
4-1	i	19.5 (0.4)	2.280 (0.012)	90.1 (1.4)	9.668E-04 (2.210E-05)
LCG541 Calibration: (0.085±0.002)x +(1.803±0.047); r2=0.976;ThO2/Th+=4.000±0.491[f]					

(a) Nomenclature indicates the grain and spot, respectively, of the analysed monazite.

(b) Monazite inclusion in garnet is designated as "i" whereas "m" indicates a matrix grain.

(c) Measured ratio in sample.

(d) Percent radiogenically derived ^{208}Pb.

(e) Corrected sample ratio assuming ^{208}Pb/^{204}Pb=39.5±0.1 (Stacey & Kramers, 1975).

(f) Calibration information: Sample name, best fit of the calibration to the equation of a line (slope*x+intercept) with ±1σ uncertainty, correlation (r^2), and range of ThO_2^+/Th+ (±1σ) measured using monazite 554 (*e.g.* Harrison *et al.*, 1999) Ideally, the unknown ThO_2^+/Th+ lies within the ThO_2^+/Th+ range defined by the standard.

in the MCT footwall show that the Sikkim MCT shear zone continued activity at various structural levels at ~10 Ma.

CONCLUSION

It can be summarised that the Daling and Darjeeling Formations of Sikkim area underwent two phases of prograde metamorphism, each culminating into a retrograde metamorphic episode. The first event was prograde regional metamorphism (M_1) during which S_1 and S_2 schistosities were formed. During this episode of metamorphism chlorite, chloritoid, biotite, garnet, staurolite and kyanite were formed. Distinct evidences have not been observed to prove whether the inverted metamorphic sequence coincides with an inversion of stratigraphic sequence. Based on metamorphic reactions, it can be stated that M/FM ratio increased during the prograde metamorphism. Most of the prograde minerals (chlorite to staurolite) in this phase of metamorphism were formed due to continuous reactions. The chemical zoning of garnets in garnet zone is normal growth type. The chemical zoning of garnets in staurolite zone show a normal growth zoning followed by an inverse chemical zoning in the outer part of core.

The results obtained by applying different geothermometers revealed temperatures upto 465 to 527°C in garnet zone and 555 to 576°C (Core parts) in staurolite zone. The maximum pressure in core parts of garnets in staurolite zone was inferred upto 6.6Kb.

The M_1 metamorphism was followed by a retrogressive phase M_{1a} due to which the prograde minerals from chlorite to kyanite were marked by alteration effects. The retrogressive effects were more dyanamic (brittle fracturing of garnet and kyanite) while at some places mylonitisation and phyllonitisation was common. The other evidences of retrogressive phase is supported by inverse chemical zoning in the outerparts of core alongwith presence of retrograded chlorite in garnet from staurolite zone; decrease of Zn in outer core parts of staurolite; penninization of chlorite; chloritisation of biotite, sericitization of feldspar and pyrophyllitisation of kyanite. The temperature and pressure of this retrogressive event are inferred from outer core parts of garnets in staurolite zone ranging from 492 to 522°C and 5.7Kb.

The prograde M_2 phase of metamorphism was primarily of burial type which later acquired a regional nature with formation of garnet, staurolite, kyanite and sillimanite (with almandine). The garnets in staurolite zone also show another prograde normal zoning varying from outer part of cores to inner parts of rim. Complete recrystallisation of garnet of low grade under high grade conditions possibly obliterated the evidences of low grade zoning in the kyanite-sillimanite zone.

Some other evidences supporting prograde metamorphism (M_2) are: (i) weak penetrative deformation and inclusion free rims of earlier multistage garnets, (ii) inclusion free and later formed idioblastic garnets and staurolite, (iii) presence of staurolite inclusion in staurolite, (iv) increase of Zn content in Fe-rich staurolite and (v) presence of K-richer muscovite, Ca-rich plagioclase and zoned K-feldspar in high grade schists and gneisses. The presence of garnet in kyanite-sillimanite zone formed during this metamorphic phase is attributed to an increase in content of Zn in staurolite which possibly acted as an internal buffer.

The temperature and pressure during M_2 phase varied from 630 to 695°C at 6.9-7.3Kb as inferred by geothermobarometric studies of kyanite-sillimanite zone. This metamorphic episode M_2 again culminated into retrograde metamorphism M_{2a}, which largely remained

confined to alteration products. During this retrogressive phase the rims of the multistage garnet were chloritised. The biotite as inclusion in the rim part of garnet showed alteration to chlorite. The other evidences are replacement of K-rich feldspar by muscovite; reverse zoning of garnet at rim, pseudomorph of chlorite after idioblastic garnet; decrease in the Zn content of staurolite and kinked and deformed cleavages in kyanite.

The studies in the Sikkim area, therefore, reveals polymetamorphic conditions of rocks. According to Staubli (1989) the Himalayan metamorphism was of Barrovian type and was of three phases. The earlier stages of metamorphism were hampered due to retrogression which affected the then formed equilibrium conditions. It records only a late retrogressive phase of polymetamorphic evolution. The polymetamorphic events in relation to deformative phases of the Daling-Darjeeling Formations of Sikkim area are suggestive of two major periods of movement of thrusting episode. The M_1 metamorphism (Barrovian) was associated with the earlier thrusting episode while M_2 phase (burial to regional) was associated with the vertical uplift followed by thrusting in later stages.

According to Sorkhabi and Stump (1993) the two phases of prograde metamorphism were Early Eocene and Early Miocene in age. It may be inferred that these two prograde metamorphic episodes in Sikkim must be related to an early Eocene and early Miocene period respectively (*cf*. Sorkhabi & Stump, 1993) whereas the retrograde metamorphic events could have occured during early middle Miocene and late Miocene period respectively (*cf* .Macfarlane *et al.* 1992).

The Late Miocene ages of Sikkim monazite grains are wholly consistent with a MCT shear zone that is active at the same time as that documented by the MBT (*e.g.*, Meigs *et al.,* 1995; Upreti, 1999). In this way, the Himalayan range does not solely follow a sequence of deformation in which convergence shifts towards the foreland as mountain building progressed, but instead records out-of-sequence thrusting. Pressure conditions recorded by the garnet rim in sample CMP860, the precise age of the monazite inclusion, and a lithostatic gradient suggest the exhumation rate of the MCT shear zone in the Sikkim region is ~2 mm yr-1 [= 6 kbar / (0.27 kbar km-1 * 10.8 Ma)], similar to that calculated for eastern Nepal (Catlos *et al.,* 2002a). The evidence suggests synchronous thrusting and out-of-sequence imbrication are mechanisms in which the Himalayan wedge maintains a critical taper (*e.g.*, Davis *et al.,* 1983, Seeber & Gornitz, 1983, Boyer, 1992). Documentation of large-scale out-of-sequence events in other contractional terrains lends further support for the feasibility of the mechanism for slip accommodation in convergent plate-tectonic settings (see Gessener *et al.,* 2001). In the Sikkim, the MCT was active at 22-20 Ma and 14-10 Ma. The in situ monazite ages from the Sikkim region are similar to ~14 Ma monazite ages found in several rocks collected ~150 km west along the Dudh Kosi-Everest transect in eastern Nepal (Catlos *et al.,* 2002a). For example, the CMP860 inclusion age of 10.8±0.3 Ma is within error of a 10.3±0.8 Ma monazite inclusion in garnet found at similar structural levels in eastern Nepal. These geochronologic results indicate the lateral continuity of orogenic events in eastern Nepal and NE India.

The MCT footwall increases in metamorphic intensity towards higher structural levels (*e.g.*, Ray, 1947), and the presence of 14-10 Ma monazite inclusions in garnet from rocks collected from the inverted sequence suggest the thrusts within the footwall shear zone juxtaposed the metamorphic sequences into their inverted position (*e.g.*, Harrison *et al.,* 1997a; 1998). Although rocks collected from the Sikkim region did not record Pliocene monazite ages as seen in central Nepal (Catlos *et al.,* 2001) and Garhwal and H. P. (Catlos, 2003),

the nappe structures in this area may obscure the reactivated ramp observed by the geometrical and structural relationship to MCT-II and MCT-III (Fig. 4) Eastern Himalaya, Sikkim. Dubey (2003) indicates that the region between the MCT-II and MCT-III is the locus of 3.5-6.8 (Mb) magnitude earthquakes since 1973-2003, leaving open the possibility that the Sikkim MCT shear zone is presently active.

ACKNOWLEDGMENTS

Authors are grateful to Dr. R.M. Manikavasgam, University of Roorkee for providing EPMA laboratary facilities and thankful to the Department of Earth and Space Sciences, University of California, Los Angles for providing Ion Microprobe facilities for Monazite dating. Authors are also grateful to Prof. S. K. Tandon and Prof. P. S. Saklani, Department of Geology, University of Delhi for valuable guidance while writing the manuscript.

REFERENCES

Acharya, S.K., 1989. The Daling group, its nomenclature, tectono-stratigraphy and structural grains: with notes on their possible equivalents. In Daling group and related rocks. *Geol. Surv. India, Spl. Publ.*, No. 22, 5-14.

Albee, A.L., 1962. Relationships between the mineral association, chemical composition and physical properties of chlorite series. *Am. Miner.*, **47**, 851-70.

Albee, A.L. & Ray, L., 1970. Correction factors for the electron probe microanalysis of silicates, oxides, carbonates, phosphates and sulfates. *Anal. Chem*., **42**, 1408-414.

Banerjee, H. & Bhattacharya, P.K., 1981. Concurrent granitisation under different metamorphic facies conditions in the lesser Himalayas of the Sikkim-Darjeeling region. *N. Jb. Miner. Abh*., **142**, 199-22.

Banerjee, P.K., Guha, P.K. & Dhiman, L.C., 1980. Inverted metamorphism in the Sikkim-Darjeeling, Himalaya. *Jour. Geol. Soc. India*, **v. 21**, 330-42.

Bell, T.H. & Johnson, S.E., 1992. Shear sense: a new approach that resolves conflicts between criteria in metamorphic rocks. *Jour. Met. Geol.*, **10**, 99-124.

Bell, T.H. & Rubenbach, M.J., 1983. Sequential porphyroblast growth and crenulation cleavage development during progressive deformation. Tectonophysics, **92**, 171-94.

Bence, A.E. & Albee, A.L., 1968. Empirical correction factors of electron microanalysis of silicates and oxides. *Jour. Geol.*, **6**, 382-03.

Berman, R.G., 1990. Mixing properties of Ca-Mg-Fe-Mn garnets. *Amer. Miner.*, **75**, 328-44.

Carmichael, D.M., 1969. On the mechanism of prograde metamorphic reactions in quartz-bearing pelitic rocks. *Contr. Miner. Petrol*., **20**, 244-67.

Catlos, E.J., Dubey2, C.S., Harrison3, T.M. & Edwards, M.A., 2003. Late Miocene Movement within the Himalayan Main Central Thrust Shear Zone, Sikkim, NE India. *Journal of Metamorphic Petrology (Communicated)*.

Catlos, E.J., Gilley, L.D., & Harrison, T.M, 2002b. Interpretation of monazite ages obtained via in situ analysis. *Chemical Geology*, **188**, 193-15.

Catlos, E.J., Harrison, T.M, Kohn, M.J., Grove, M., Ryerson F.J., Manning, C.E., & Upreti, B.N., 2001. Geochronologic and thermobarometric constraints on the evolution of the Main Central Thrust, central Nepal Himalaya. *Journal of Geophysical Research*, **106**, 16177-6204. 19.

Catlos, E.J., Harrison, T.M, Manning, C.E., Grove, M., Rai, S.M., Hubbard, M.S., & Upreti, B.N., 2002a. Records of the evolution of the Himalayan orogen from in situ Th-Pb ion microprobe dating of monazite: Eastern Nepal and Garhwal. *Journal of Asian Earth Sciences*, **20**, 459-79.

Catlos, E.J, Harrison, T.M., Dubey, C.S. & Edwards, M.A., 2002c. P-T-t constrains on the evolution of the Sikkim Himalaya. *Jour. Asian Earth Sc.* (Special Abstract Issue, 17th HKT Workshop, Gangtok, Sikkim, India) **vol. 20**, No. 4A, 6-7.

Chinner, G.A., 1965. The kyanite isograd in Glen Clova, Angus, Scotland. *Miner. Mag.*, **34**, 132-43.

Crawford, M.L., 1974. Calcium zoning in almandine: a model based on plagioclase equilibria. In: The Feldspars (Ed. Mackenzie, W.S. & Zussman, J.), Manchester University Press, Manchester, 629-44.

——1977. Calcium zoning in almandine garnet, Wissahickon Formation, Philadelphia, Pennsylvania. *Canadian Miner.*, **15**, 243-49.

Cygan, R. & Lasaga, A.C., 1982. Crystal growth and formation of chemical zoning in garnets. *Contr. Miner. Petrol.*, **79**, 187-200.

Das, B.K., 1987. Petrology of Barrovian type regional metamorphism in pelitic schists of Kishtwar, Kashmir Himalayas, India. *Proc. Nat. Sem. Tert.*, Orogeny, 153-87.

De Bethune, P., Laduron D. & Bocquet, J., 1975. Diffusion processes in resorbed garnets. *Contr. Miner. Petrol.*, **50**, 197-04.

Dempster, J., 1985. Garnet zoning and metamorphism of Barrovian type area, Scotland. *Contr. Miner. Petrol.*, **89**, 30-38.

Dhana Raju, R., Satyanarayana, B. & Krishna Rao, J.S.R., 1977. Variation of MnO and TiO_2 contents of biotite in relation to metamorphic grade. *Ind. Jour. Earth Sci.*, **4**, 13-19.

Dietvorst, E.J.L., 1982. Retrograde garnet zoning at low water pressure in metapelitic rocks from Kemio, SW Finland. *Contr. Miner. Petrol.*, **79**, 37-45.

Dubey, C.S., 1993. Study of the lesser Himalayan metamorphics, Eastern Sikkim, India. Ph.D. Thesis (unpublished), 151.

Eggleton, R.A. & Banfield, J.F., 1985. The alteration of granitic biotite to chlorite. *Am. Miner.*, **70**, 902-910.

Ferry, J.M. & Spear, F.S., 1978. Experimental calibration of the partitioning of Fe and Mg between biotite and garnet. *Contr. Miner. Petrol.*, **66**, 113-117.

Frey, M., 1974. Alpine metamorphism of pelitic and marly rocks of the Central Alps. *Schweiz. Mineral. Petrogr. Mitt.*, **54**, 489-06.

Ganguly, J., Dasgupta, S., Cheng, W. & Neogi, S., 2000. Exhumation history of a section of the Sikkim Himalayas India: records in the metamorphic mineral equilibria and compositional zoning of garnet. *Earth and Planetary Science Letters*, **183**, 471-86.

Ghent, E.D. & Stout, M.Z., 1981. Geobarometry and geothermometry of plagioclase-biotite-garnet- muscovite assemblages. *Contr. Miner. Petrol.*, **76**, 92-97.

Ghose, N.C., 1979. Hydrothermal melting relationship of some high grade metamorphic rocks of Darjeeling. In: *Metamorphic rock sequences of the Eastern Himalaya*, (Ed. P.K. Verma) K.P. Bagchi and Co. Calcutta, 139-49.

Goff, E.L. & Ballevre, M., 1990. Geothermobarometry in Albite- garnet orthogneisses: a case study from Gran Paradiso nappe (Western Alps). *Lithos*, **25**, 261-80.

Grant, J.A. & Weiblen, P.W., 1971. Retrograde zoning in garnet near the 2nd sillimanite isograd. *Amer. Jour. Sci.*, **270**, 281-96.

Guidotti, C.V., 1969. A comment on 'chemical study of minerals from the Moine schists of the Ardnamurchan area, Argyllshire, Scotland and its implications for the phengite problem. *Jour. Petrol.*, **10**, 164-70.

——1974. Transition from staurolite to sillimanite zone, Rangeley Quadrangle, Maine. Bull. *Geol. Soc. Amer.*, **85**, 475-90.

——1984. Micas in Metamorphic rocks. In: Micas: Mineralogical Society of America, (Ed. S.W. Bailey), *Rev. in Miner.*, **13**, 435-467.

Guidotti, C.V., Cheney, J.T., & Henry, D.J., 1988. Compositional variation of biotite as a function of metamorphic reactions and mineral assemblage in the pelitic schists of Western Maine. *Amer. Jour. Sci.*, 288-A, 270-92.

Harrison, T.M., Grove M., Lovera O.M. & Catlos E.J., 1998. A model for the origin on Himalayan anatexis and inverted metamorphism. *Journal of Geophysical Research*, **103**, 27017-7032.

Harrison, T.M., Grove, M., McKeegan, K.D., Coath, C.D., Lovera, O.M. & Le Fort, P., 1999. Origin and emplacement of the Manaslu intrusive complex, Central Himalaya. *Journal of Petrology,* **40**, 3-19.

Harrison, T.M., Ryerson, F.J., Le Fort, P., Yin, A., Lovera, O.M. & Catlos, E.J., 1997a. A Late Miocene-Pliocene origin for central Himalayan inverted metamorphism. *Earth and Planetary Science Letters*, **146**, E1-E8.

Hess, P.C., 1971. Prograde and retrograde equilibrium in Garnet- cordierite gneisses in the south-central Massachussets. *Contr. Miner. Petrol.*, **30**, 177-95.

Hodges, K.V. & Spear, F.S., 1982. Geothermometry, geobarometry and the Al_2SiO_5 triple point at Mt. Moosilauke, New Hampshire. *Amer. Miner.*, **67**, 1118-134.

Hoisch, T.D., 1990. Empirical calibration of six geobarometers for the mineral assemblage quartz + muscovite + biotite + plagioclase + garnet. *Contr. Miner. Petrol.*, **104**, 225-34.

Hollister, L.S., 1966. Garnet zoning and interpretation based on the Rayleigh fractionation model. *Science*, **154**, 647-651.

Hyndman, D.W., 1985. Petrology of igneous and metamorphic rocks - McGraw Hill, New York.

Johnson, S.E., 1990. Deformational history of the Otago schists, New Zealand, from progressive developed phorphyroblast/matrix microstructures: cyclic uplift-collapse orogenesis and its implications. *Jour. Struct. Geol.*, **12**, 727-746.

Karabinos, P., 1984. Polymetamorphic garnet zoning from Southeastern Vermount. *Amer. Jour. Sci.*, **284**, 1008-025.

Kerr, A., 1981. Zoning in Garnet from the mainland Lewisian. *Miner. Mag.*, **44**, 919-994.

Krogh, E.J. & Raheim, A., 1978. Temperature and pressure dependence of Fe-Mg partitioning between garnet and phengite, with particular reference to eclogites. *Contr. Miner. Petrol.*, **66**, 75-80.

Labotka, T.C., 1980. Petrology of a medium pressure regional metamorphic terrain, Funeral Mountains, California. *Amer. Miner.*, **65**, 670-89.

Laird, J., 1989. Chlorites: Metamorphic petrology. In: Hydrous phyllosilicates, Mineralogical Society of America. *Rev. in miner.*, **19**, 405-53.

Lal, R.K., Mukherjee, S. & Ackermand, D., 1981. Deformation and Barrovian metamorphism at Takdah, Darjeeling (Eastern Himalaya). In: *Metamorphic tectonites of the Himalaya* (Ed. P.S. Saklani), 231-78.

Lasaga, A.C., Richardson, S.M. & Holland, H.D., 1977. The mathematics of cation diffusion and exchange between silicate minerals during retrograde metamorphism. In: *Energetics of geological processes.* (Ed. S.K. Saxena & S. Bhattacharji), Springer Verlag, New York, 353-88.

Liou, J.G., 1973. Synthesis and stability relations of epidote, $Ca_2Al_2FeSi_3O_{12}(OH)$, *Jour. Petrol.*, **14**, 381-13.

Macfarlane, A.M., Hodges, K.V. & Lux, D., 1992. A structural analysis of the Main Central Thrust zone, Langtang National Park, central Nepal Himalaya. Bull. *Geol. Soc. Amer.*, **104**, 1389-402.

Miyashiro, A. & Shido, F., 1985. Tschermak substitution in low-and middle-grade pelitic schists. *Jour. Petrol.*, **26**, 449-87.

Mohan, A., Windley, B.F. & Searle, M.P., 1989. Geothermobarometry and development of inverted metamorphism in Darjeeling-Sikkim region of the Eastern Himalaya. *Jour. Met. Geol.*, **7**, 95-110.

Neogi, S., Dasgupta, S. & Fukuoka, M., 1998. High P-T polymetamorphism, dehydration melting, and generation of migmatites and granites in the Higher Himalayan crystalline complex, Sikkim, India. *Journal of Petrology*, **39**, 61-99.

Newton, R.C. & Haselton, H.T., 1981. Thermodynamics of the garnet - plagioclase - Al_2SiO_5 quartz geobarometer. In: *Thermodynamics of mineral and melts* (Ed. R. C. Newton *et al.*), Springer-Verlag, New York, 131-147.

Robinson, P., Tracy R.J. & Pomeroy, J.S., 1977. High pressure sillimanite garnet biotite assemblage formed by recrystallisation of mylonite in sillimanite-cordiertie- orthoclase schist, Central Massachusetts. *Geol. Soc. Amer. (Abst. with progr.)*, **9**, 1144-145.

Ruiz, J.L., Apparicio, A. & Cacho, L.G., 1978. Chemical variation in biotites during prograde metamorphism, Sierra De Guadarrama, Sistema Central, Spain. *Chem. Geol.*, **21**, 113-29.

Saklani, P.S., 1993. Geology of the Lower Himalaya (Garhwal). International Book and Periodicals, Delhi, 241.

Schreurs, J., 1985. Prograde metamorphism of metapelites garnet- biotite thermometry and prograde changes of biotite chemistry in high grade rocks of West Uusimaa, Southwest Finland. *Lithos*, **18**, 69-80.

Sinha Roy, S., 1977. Metamorphism and tectonics of the Himalayas, as illustrated in the Eastern Himalayas. *Geotectonics*, **v. 11**, no. 2, 120-124.

Sorkhabi, R.B. & Stump, E., 1993. Rise of the Himalaya: A geochronologic approach. *GSA Today*, **3**, 85-92.

Spear, F.S., 1981. Amphibole-plagioclase equilibria: An empirical model for the relation Albite + Tremolite = Edenite + Quartz. *Contr. Miner. Petrol.*, 77, 355-64.

Spear, F.S. & Peacock, S.M., 1990. Metamorphic P-T-t paths. Program manual and computer exercises for the calculation of metamorphic phase equilibria, pressure-temperature-time paths and thermal evolution of orogenic belts. Deptt. of Geology, Arizona State University, Tempe, U.S.A.

Staubli, A., 1989. Polyphase metamorphism and the development of the Main Central Thrust. *Jour. Met. Geol.*, **7**, 73-94.

Thompson, A.B., 1976. Mineral reactions in pelitic rocks: 1. Prediction of P-T-X (Fe-Mg) phase relations. *Amer. Jour. Sci.*, **276**, 401-24.

Thompson, A.B., Tracy, R.J., Lyttle, P. & Thompson, J.B. Jr., 1977. Prograde reaction histories deduced from compositional zonation and mineral inclusions in garnets from Gassette schist. Vermont. *Amer. Jour. Sci.*, **277**, 1152-167.

Thompson, J.B. Jr. & Norton, S.A., 1968. Paleozoic regional metamorphism in New-England and adjacent areas. In: *Studies of Appalachian Geology* (Ed. Zen, E-an *et al.*). Northern and Maritime New York. Interscience, 319-29.

Tracy, R.J., 1982. Compositional zoning and inclusions in metamorphic minerals. In: Characterisation of metamorphism through mineral equilibria (Ed. J.M. Ferry), Mineralogical Society America, *Rev. in Miner.*, **10**, 355-97.

Tracy, R.J., Robinson, P. & Thompson, A.B., 1976. Garnet composition and zoning in determination of temperature and pressure of metamorphism, Central Massachusetts. *Amer. Miner.*, **61**, 762-75.

Vernon, R.H. & Flood, R.H., 1979. Microstructural evidence of time relationships between metamorphism and deformation in the metasedimentary sequence of the Northern Hill End Trough, New South Wales, Australia. *Tectonophysics*, **50**, 127-137.

Winkler, H.G.F., 1979. Petrogenesis of metamorphic rocks. Springer-Verlag, New York.

Zwart, H.J., 1960. The chronological succession of folding and metamorphism in the Central Pyrenees. *Geol. Rundsch.*, **50**, 203-218.

Zwart, H.J., 1962. On the determination of polymetamorphic mineral associations and its application to the Bosost area (Central Pyreenes). *Geol. Rundsch.*, **52**, 38-65.